Journal of Organometallic Chemistry, 391 (1990) 81–107
Elsevier Sequoia S.A., Lausanne – Printed in The Netherlands
JOM 20795

Cluster chemistry

LXIII *. Further studies of the thermal behaviour of $\{Ru_3(CO)_{11}\}_2(\mu$-dppa) (dppa = $C_2(PPh_2)_2$). Crystal structures of $Ru_4(\mu_4$-PPh)$(\mu_4$-$PhC_2PPh_2)(\mu$-CO$)_2(CO)_8 \cdot$ MeOH, $Ru_5(\mu_4$-PPh$)\{\mu_3$-CCPh$(PPh_2)\}(CO)_{12}$, $Ru_5(\mu_3$-H$)(\mu_4$-PPh$)\{\mu_4$-CCPh$(C_6H_4)\}(\mu_3$-PPh$)(CO)_{10}$ and $Ru_5(\mu_4$-PPh$)\{\mu_4$-CCPh$(C_6H_4)\}\{\mu$-PPh(OMe)$\}(CO)_{11} \cdot 2$MeOH $\cdot H_2O$

Michael I. Bruce *, Michael J. Liddell and Edward R.T. Tiekink

Jordan Laboratories, Department of Physical and Inorganic Chemistry, University of Adelaide, Adelaide, South Australia 5001 (Australia)

(Received January 29th, 1990)

Abstract

Large scale (ca. 2 g) preparations of $Ru_5(\mu_5$-$C_2PPh_2)(\mu$-$PPh_2)(CO)_{13}$ (**2**) by pyrolysis of $\{Ru_3(CO)_{11}\}_2(\mu$-dppa) have also afforded the complexes $Ru_4(\mu_4$-PPh$)(\mu_4$-$PhC_2PPh_2)(\mu$-CO$)_2(CO)_8$ (**3**), $Ru_5(\mu_5$-$C_2PPh_2)(\mu$-$PPh_2)(CO)_{15}$ (**4t**), $Ru_4(\mu_4$-$C_2)(\mu$-$PPh_2)_2(CO)_{12}$ (**5**), $Ru_5(\mu_4$-PPh$)\{\mu_3$-CCPh$(PPh_2)\}(CO)_{12}$ (**6**) and $Ru_5(\mu$-H$)(\mu_4$-PPh$)\{\mu_4$-CCPh$(C_6H_4)\}(\mu_3$-PPh$)(CO)_{10}$ (**7**). The new complexes **6** and **7**, identified crystallographically, are formed by heating **2**; the evolved CO reacts with **2** to give **4t** and **7**. Complex **6** contains a square pyramidal Ru_5 core, the square face being capped by PPh, and a triangular face by the phosphino-vinylidene ligand, which is formed by migration of Ph from P to C_β of the C_2PPh_2 ligand in **2**. Complex **7** contains a $CPRu_5$ pentagonal bipyramid, with PPh capping an Ru_3 face. Complex **7** reacts with MeOH to give $Ru_5(\mu_4$-PPh$)\{\mu_4$-CCPh$(C_6H_4)\}\{\mu$-PPh(OMe)$\}(CO)_{11}$ (**12**), with the same core as **7**; the μ_3-PPh group has been converted to a μ-phosphido ligand. In **7** and **12**, the organic fragment is a metallated diphenylvinylidene. Some ^{31}P NMR data for these and related complexes are given and discussed. The crystal structure of **3** as its methanol solvate is also reported.

---

* For part LXII see ref. 1.

Introduction

Previous papers have described the synthesis of $\{Ru_3(CO)_{11}\}_2(\mu\text{-dppa})$ (dppa = $C_2(PPh_2)_2$) (**1**; Scheme 1) and its high yield conversion to the open pentanuclear cluster $Ru_5(\mu_5\text{-}C_2PPh_2)(\mu\text{-}PPh_2)(CO)_{13}$ (**2**) [2]. The latter complex is very reactive and we have described reactions with CO or H_2; products containing altered metal skeletons and modified ligands have resulted [3,4]. A brief review of this chemistry has been given [5].

The easy accessiblity of **2** has prompted a more detailed study of its chemistry. In the course of optimising the synthesis of **2** (see Experimental), we have discovered several interesting by-products in the preparation, and have clarified the mode of formation of some of them. This paper describes this chemistry, together with the crystal structures of two of the complexes isolated, and summarises some ^{31}P NMR data obtained for these and related complexes.

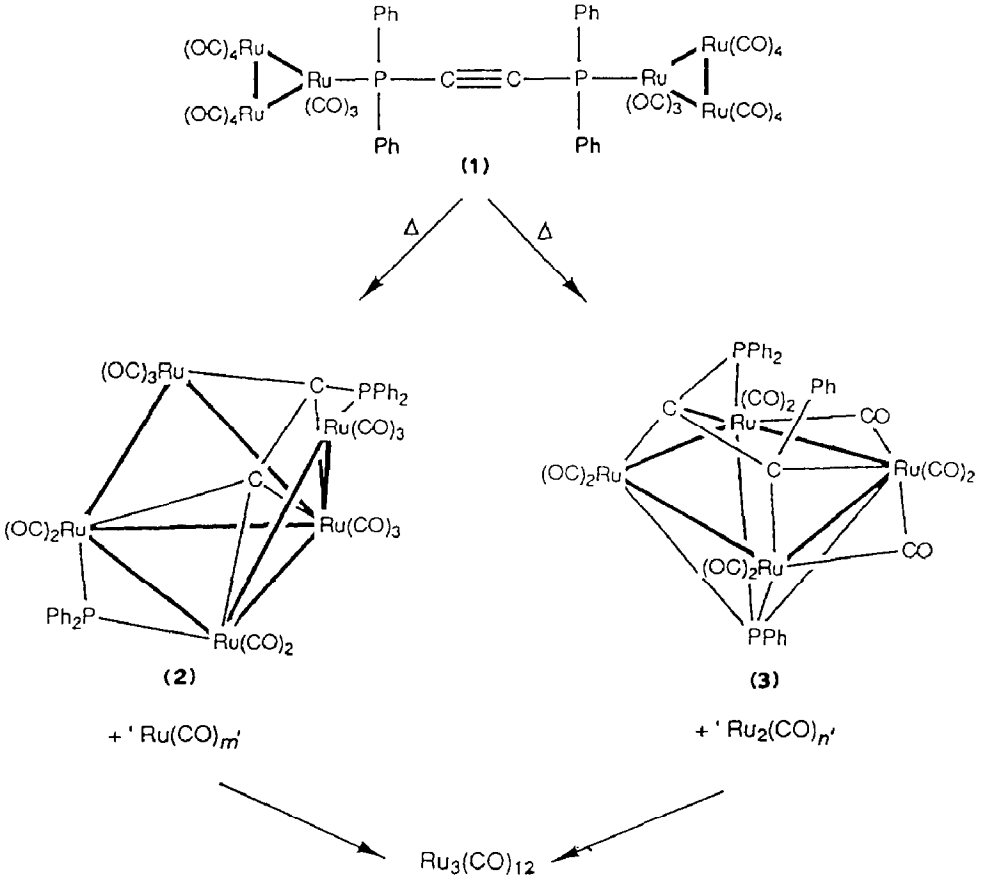

Scheme 1. Synthesis of **2** and **3** from **1**.

Results and discussion

Further observations on the synthesis of $Ru_5(\mu_5\text{-}\eta^2,P\text{-}C_2PPh_2)(\mu\text{-}PPh_2)(CO)_{13}$ (2)

When the synthesis of **2** from $\{Ru_3(CO)_{11}\}_2(\mu\text{-dppa})$ was performed on a gram scale, a variety of products was obtained in addition to **2**. The major complexes isolated and identified were: **2**, $Ru_4(\mu_4\text{-PPh})\{\mu_4\text{-}\eta^2,P\text{-}PhC_2PPh_2\}(\mu\text{-CO})_2(CO)_8$ (**3**) [6], $Ru_5(\mu_5\text{-}\eta^2,P\text{-}C_2PPh_2)(\mu\text{-}PPh_2)(CO)_{15}$ (**4t**) [3], $Ru_4(\mu_4\text{-}\eta^2\text{-}C_2)(\mu_3\text{-}PPh_2)_2(CO)_{12}$ (**5**) [4b], $Ru_5(\mu_4\text{-PPh})\{\mu_3\text{-}\eta^2,P\text{-CCPh}(PPh_2)\}(CO)_{12}$ (**6**) and $Ru_5(\mu\text{-H})(\mu_4\text{-PPh})\{\mu_4\text{-}\eta^4\text{-CCPh}(C_6H_4)\}(\mu_3\text{-PPh})(CO)_{10}$ (**7**). Complexes **6** and **7** were also obtained by pyrolysis of **2**. The relative yields of the products could be varied by altering reaction parameters such as temperature and time and by controlling the reaction atmosphere. Most critical of these parameters was the pyrolysis temperature for the conversion of $\{Ru_3(CO)_{11}\}_2(\mu\text{-dppa})$ to **2**. If the temperature was increased from 90 °C to 111 °C, the major products formed were $Ru_3(CO)_{12}$, **2**, **5**, **6** and **7**. Two orange clusters were also observed, and were formulated as $Ru_8(CO)_{17}(dppa^*)$ * and $Ru_5(CO)_{13}(dppa^*)$. If the duration of the reflux was increased (from 90 min to 3 h), as well as the temperature, then significant proportions of complexes **6** and **7** were formed. If the conversion was not performed with a N_2 purge, the evolved CO reacted with **2** under the pyrolysis conditions to form the clusters $Ru_5(\mu_5\text{-}\eta^2,P\text{-}C_2PPh_2)(\mu\text{-}PPh_2)(CO)_{15}$ (**4t**) and $Ru_4(\mu_4\text{-}\eta^2\text{-}C_2)(\mu\text{-}PPh_2)_2(CO)_{12}$ (**7**). Both these clusters have been synthesized previously in the reactions of **2** with CO [3]. Separation of **3** and **4t** from **2** on a large scale was found

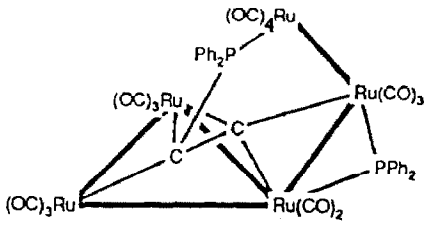

(4k)

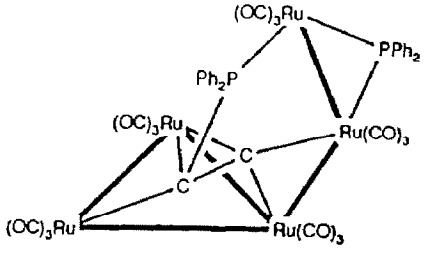

(4t)

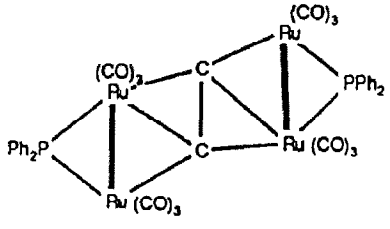

(5)

* (dppa*) is used throughout this paper to indicate the incorporation of the elements of dppa in the cluster; the ligand does not necessarily correspond to structurally intact dppa.

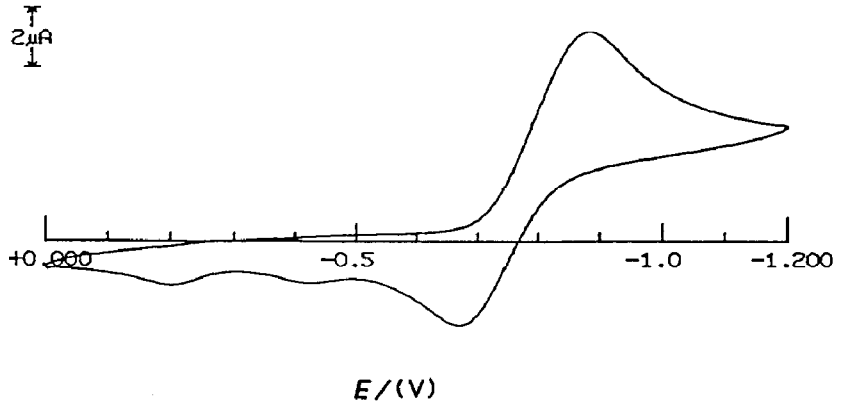

Fig. 1. Cyclic voltammogram of **2** (CH_2Cl_2; 200 mV s^{-1}).

to be difficult, so the reaction conditions had be carefully controlled in order to avoid low yields of **2**.

New spectroscopic data have been obtained for **2**. The fast atom bombardment (FAB) mass spectrum showed a molecular ion and ions formed by sequential loss of 13 carbonyl groups. After prolonged periods in the FAB beam, ions at m/z 1321 and 1293 corresponding to $Ru_5(CO)_n(dppa^*)$ ($n = 15$, 14) were observed. These have the same nominal mass as ions noted in the spectra of **4k** and **4t** (see below) and suggest that intermolecular reactions such as CO transfer are occurring in the matrix or in the selvage region directly above the surface of the matrix [7]. Generally, such reactions have not proved a problem in the examination of these cluster complexes, except when particularly labile ligands were present. The FAB mass spectra for **4t** and **4k** were identical and showed molecular ions at m/z 1321 and ions formed by stepwise loss of 15 carbonyl groups.

The ^{13}C NMR spectrum of **2** suggested that several of the carbonyl ligands are either fluxional at room temperature [1] or are accidentally equivalent, as only nine signals were found between δ 202.5 and 192.5 in contrast to the 13 CO environments expected from the C_1 symmetry of **2** [2]. The chemical shifts noted for C^α and C^β at δ 239.0 (doublet, J(PC) 23 Hz) and 108.8 (doublet, J(PC) 22 Hz), respectively, are similar to those found for other μ_4-η^2-acetylide complexes [8]. The α-carbon is particularly electron-deficient and should be susceptible to nucleophilic attack.

An electrochemical study of **2** was carried out to determine whether a stable anion could be generated. A cyclic voltammogram at 200 mV s^{-1} is shown in Fig. 1. The process was quasi-reversible with $E_{1/2}$ −0.78 V, suggesting that it should be possible to reduce **2** chemically with a reagent such as sodium amalgam ($E_{1/2}$ −2.0 V DMF) [9]. Treatment of **2** with sodium amalgam gave black solution, which had ν(CO) bands at 2021(sh), 2005(sh), 1968vs and 1948(sh) cm^{-1}. It has not been possible to isolate a product from this reduced solution. Treatment of the reduced solution with [ppn]Cl in MeCN resulted in further reaction, and the anion so obtained gave an IR spectrum different from that of the original reduced solution. A FAB mass spectrum of the ppn salt of this anion showed a molecular negative ion $[M]^-$ at m/z 1236, which corresponds to $[Ru_5(CO)_{12}(dppa^*)]^-$ (this does not rule out the possibility of ions such as $[Ru_5H(CO)_{12}(dppa^*)]^-$ being formed from $[Ru_5(CO)_{12}(dppa^*)]^{2-}$ in the spectrometer).

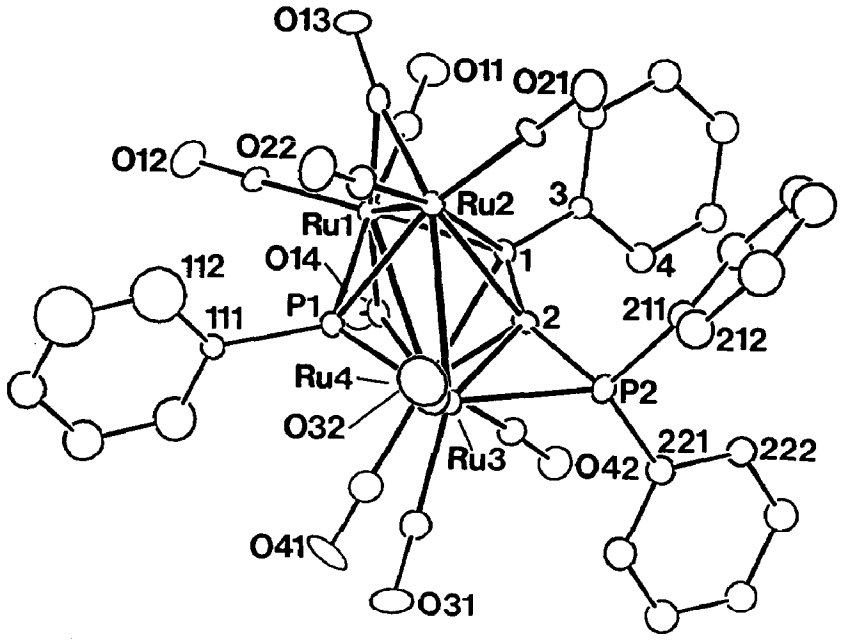

Fig. 2. ORTEP view of $Ru_4(\mu\text{-PPh})(\mu_4\text{-PhC}_2\text{PPh}_2)(\mu\text{-CO})_2(CO)_8$ (3) showing atom-labelling scheme. Atoms not otherwise indicated are carbons. Note that Ru(4) is obscured under CO(32).

At this stage it is not clear whether the product formed initially is a '$(CO)_{12}$' or '$(CO)_{13}$' species, or whether it is a monoanion or a dianion. Some indirect evidence has been gained from the addition of two $Au(PPh_3)$ units to the anion in its reaction with $AuCl(PPh_3)$, which suggests that the $[Ru_5(CO)_{12}(dppa^*)]^{2-}$ formulation may be correct. The appearance of the small anodic waves at E −0.43 V and −0.20 V suggest that CO loss or skeletal changes may occur [11,12]. An attempt to initiate an ETC reaction between **2** and dppa using sodium diphenyl ketyl (Na/bpk) catalyst was unsuccessful.

Complex **3** gave a FAB mass spectrum which showed a molecular ion at m/z 1080 which fragmented by stepwise loss of ten carbonyl groups. In conjunction with analytical, ^{1}H NMR and ^{31}P NMR data a formulation similar to that reported by Daran et al. [6] for the complex $Ru_4(\mu_4\text{-PPh})\{\mu_4\text{-}\eta^2,P\text{-PhC}_2\text{PPh}_2\}(\mu\text{-CO})_2(CO)_8$ was indicated. The IR data reported for their complex (2065w, 2030vs, 1985(sh), 1980s, 1970s, 1842vs cm^{-1}) were significantly different from that obtained for **3** (2061w, 2030vs, 2008m, 2001w, 1982w, 1964w, 1878vw, 1851w cm^{-1}). An X-ray crystallographic study was therefore carried out on **3**, to determine whether a structure different to that reported by Daran et al. [6] was present. However, it was found to be identical, except for the presence of a molecule of solvated MeOH in our sample (this altered the unit cell dimensions). Separation of clusters with R_f values similar to **3** could not be achieved under the column chromatography conditions specified by Daran et al. [6] and co-crystallization of **3** with other Ru_5 clusters (e.g. **2**, **4t**) occurs readily, which probably accounts for the major differences in the IR spectra noted above. An ORTEP plot of a molecule of **3** is shown in Fig. 2. In the redetermination of the structure **3**, the greatest variation in bond lengths was found for Ru(2)–C(2) 2.429(9) Å (Lit. [6] 2.310(8) Å); most other differences are within 3 esd's. A cluster with a related geometry, $Ru_4\{\mu_4\text{-}\eta^3\text{-P(Ph)CHCH}\}(\mu_4$-

PPh)(μ-CO)(CO)$_{10}$, has been synthesized recently by insertion of acetylene into the Ru–P bonds of a phosphinidene group in Ru$_4$(μ_4-PPh)$_2$(μ-CO)(CO)$_{10}$ [10].

It appears that **3** is formed through condensation of **1** under a slight CO partial pressure, as small amounts of **3** were always recovered in the synthesis of **2**, even with a nitrogen purge. A bimolecular process may be involved whereby the lost 'Ru$_2$(CO)$_n$' fragment formed in the synthesis of **3** combines with the lost 'Ru(CO)$_m$' fragment formed in the synthesis of **2** to form Ru$_3$(CO)$_{12}$ (see Scheme 1).

In terms of polyhedral skeletal electron pair (PSEP) theory, **3** is a 62-electron, 7-SEP cluster, the phosphino-alkyne interacting with all four metal atoms on the square face, acting as a six-electron donor through the phosphorus atom and the alkyne. Although MO calculations have indicated that the electron-precise 64-electron, 8-SEP configuration is favoured for iron systems, examples of this type of complex, such as Fe$_4$(μ_4-PPh)$_2$(CO)$_{11}$(L) (L = CO, PR$_3$) lose CO reversibly to give Fe$_4$(μ_4-PPh)$_2$(CO)$_{10}$(L) [11,12]. The ruthenium analogues are expected to form only the 62-electron species; Ru$_4$(μ_4-PPh)$_2$(CO)$_{11}$, for example, does not add CO to give the 8-SEP cluster [13].

The direct synthesis of **5** from **2** was attempted in the hope of increasing the yield of this compound, which contains a μ_4-η^1,η^2-ethynediyl dianion (C_2^{2-}). In fact, the yield by this route (11%) was lower than that previously obtained (28%) [4b]. Further spectroscopic data has been collected for **5**. The FAB mass spectrum showed a molecular ion at *m/z* 1137, which fragments by sequential loss of twelve CO groups. A ^{13}C NMR spectrum contained three resonances for the CO groups (all multiplets). As the molecule displays C_2 symmetry, six unique CO sites are expected. The signals observed, therefore, indicate either accidental equivalence of signals or that carbonyl exchange processes are occurring. The doublet at δ 141.1 (J(PC) 37 Hz) was assigned to the carbons of the C_2 fragment and suggests that both carbons are equivalent and that each carbon is coupled to only one phosphorus. Carty et al. [8] have shown that the C_α resonances have quite large ^{31}P-^{13}C couplings (J(PC) 27.4–27.8 Hz) for Ru$_2$(μ_2-η^2-C$_2$R)(μ-PPh$_2$)(CO)$_6$ (R = Ph, Bu^t), whereas C$^\beta$ couplings are in the range 7.7–8.0 Hz.

Pyrolysis of 2

In the course of studying the pyrolytic behaviour of **2**, we isolated Ru$_5$(μ_4-PPh){μ_3-η^2,*P*-CCPh)}(CO)$_{12}$ (**6**) and Ru$_5$(μ_3-H)(μ_4-PPh){μ_4-η^4-CCPh(C$_6$H$_4$)}(μ_3-PPh)(CO)$_{10}$ (**7**). Both these complexes have been fully characterized by X-ray studies. Plots of the two molecular structures are shown in Fig. 3 and 4, and significant bond distances and angles are collected in Tables 1 and 2. Complexes **6** and **7** were formed sequentially when **2** was heated in toluene. After 2.5 h at reflux, complex **6** was isolated in 22% yield as a brown crystalline material and complex **7** in > 65% yield as a dark green crystalline material.

The IR spectrum of **6** had an seven-band all-terminal ν(CO) pattern. No cluster-bound hydride resonances were found in the ^{1}H NMR spectrum, which contained resonances for the phenyl groups between δ 7.9 and 6.8. In the ^{13}C NMR spectrum of complex **6**, only four CO signals were found at δ 202.6, 197.0, 192.6 and 192.3. The C$^\alpha$ (δ 148.8, d, J(PC) 15 Hz) and the C$^\beta$ (δ 109.2, multiplet) signals were in environments similar to those of other μ_3-η^2-acetylide cluster complexes [8]. The FAB mass spectrum showed a molecular ion at *m/z* 1236 which fragmented by stepwise loss of ten CO groups.

Table 1

Selected bond lengths (Å) for **6**

Ru(1)–Ru(3)	2.776(4)	Ru(1)–Ru(4)	2.961(5)
Ru(1)–Ru(5)	2.826(5)	Ru(2)–Ru(3)	2.874(5)
Ru(2)–Ru(4)	2.870(5)	Ru(2)–Ru(5)	2.808(5)
Ru(3)–Ru(5)	2.832(6)	Ru(4)–Ru(5)	2.810(5)
Ru(1)–P(1)	2.44(1)	Ru(2)–P(1)	2.38(1)
Ru(3)–P(1)	2.36(1)	Ru(4)–P(1)	2.36(1)
Ru(1)–P(2)	2.33(1)	Ru(3)–C(19)	2.24(5)
Ru(1)–C(20)	2.08(4)	Ru(3)–C(20)	2.15(4)
Ru(5)–C(20)	1.88(5)	P(2)–C(19)	1.84(5)
C(19)–C(20)	1.45(6)		

The X-ray structure of **6** is of limited accuracy, but determines unambiguously the stereochemistry of this cluster complex. Figure 3 shows that the five Ru atoms in **6** form a square pyramid, the square face of which is capped by a PPh group, equidistant from Ru(2), Ru(3) and Ru(4) ($Ru–P_{av}$. 2.37 Å, $RuPRu_{av}$. 74.6°) but somewhat further away from Ru(1) (2.44(1) Å). The phosphinovinylidene ligand is asymmetrically coordinated: C(20) is displaced towards Ru(3) (Ru(3)–C(20) 1.88(3) Å), while C(19) interacts rather weakly with Ru(3) (Ru(3)–C(19) 2.24(3) Å). The C=C bond length (1.45(6) Å) is typical of cluster-bound vinylidenes [14]. Several carbonyls are bent (RuCO 163–169°C); these appear to reflect steric interactions within the cluster, since the Ru–C distances are clearly non-bonding (> 3.0 Å). In terms of SEP electron counting, **6** is a 7-SEP, 74-electron *nido*-octahedral cluster.

Cluster **6** is formed from **2** by P–C bond cleavage and phenyl migration to the acetylide, which generates a phosphino-vinylidene. Contraction of the open Ru_5 cluster found in **2** to the square-pyramidal arrangement in **6** occurs as a result of the loss of one CO ligand. A similar transformation occurs when $Ru_5(\mu_4\text{-}\eta^2\text{-}C_2Ph)(\mu\text{-}PPh_2)(CO)_{14}$ (**8**) is warmed [15]. Formation of the $CCPh(PPh_2)$ ligand occurs by formal cluster-assisted transfer of a phenyl group from the μ-PPh_2 group in **2** to the β-carbon of the phosphinoacetylide. Consideration of the Ru–C distances, particularly Ru(3)–C(20) and Ru(3)–C(19) (see above), suggests that a tautomeric methylidyne form of the ligand may also be contributing to the structure. This suggestion

Table 2

Selected bond lengths (Å) for **7**

Ru(1)–Ru(2)	3.065(1)	Ru(1)–Ru(3)	2.874(1)
Ru(1)–Ru(4)	2.840(1)	Ru(2)–Ru(3)	2.895(1)
Ru(2)–Ru(4)	3.605(1)	Ru(2)–Ru(5)	2.743(1)
Ru(3)–Ru(4)	2.855(1)	Ru(4)–Ru(5)	2.854(1)
Ru(1)–P(1)	2.300(3)	Ru(2)–P(1)	2.488(3)
Ru(4)–P(1)	2.479(3)	Ru(5)–P(1)	2.326(3)
Ru(1)–P(2)	2.280(3)	Ru(3)–P(2)	2.243(3)
Ru(4)–P(2)	2.273(3)	Ru(2)–C(11)	2.14(1)
Ru(3)–C(11)	2.09(1)	Ru(4)–C(11)	2.37(1)
Ru(5)–C(11)	2.25(1)	Ru(5)–C(12)	2.26(1)
Ru(5)–C(13)	2.33(1)	Ru(5)–C(14)	2.23(1)
C(11)–C(12)	1.41(2)		

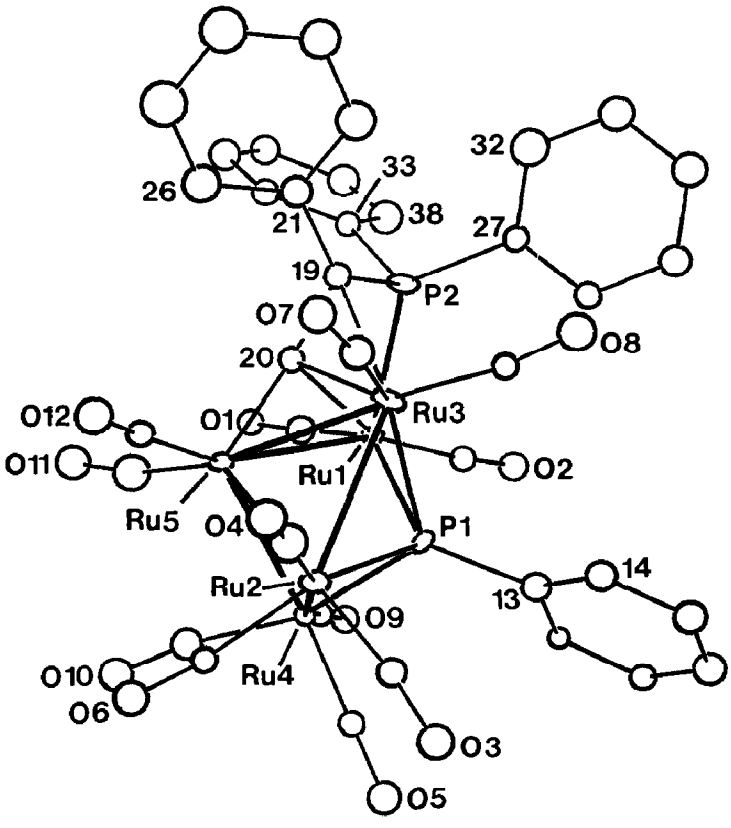

Fig. 3. ORTEP view of $Ru_5(\mu_4\text{-PPh})\{\mu_3\text{-CCPh}(PPh_2)\}(CO)_{12}$ (**6**) showing atom-labelling scheme. Atoms not otherwise indicated are carbons.

is supported by the close resemblance of the structure of **6** to that of $Ru_5(\mu_4\text{-PPh})(\mu_3\text{-CCH}_2Pr^i)(\mu\text{-PPh}_2)(CO)_{12}$ (**9**) [16], which contains an alkylidyne capping a triangular face of a square pyramid. The formation of phosphinidene groups through phenyl loss has been noted previously [17], and the migration of phenyl groups from phosphorus to carbon has been recognized as a metal-assisted process [18]. To our knowledge, however, this is the first occasion on which migration of a phenyl group from P to C to generate a vinylidene ligand has been demonstrated (see Scheme 2). Related compounds containing cluster-bound alkynes have already been synthesized, examples being **5** [6] and $Ru_5(\mu_4\text{-PPh})(\mu_3\text{-}\eta^2\text{-PhC}_2\text{Ph})(CO)_{13}$ (**10**) [17].

In the IR spectrum of **7**, eight ν(CO) bands were found in the terminal region. A hydride resonance was found at δ −15.38 (dd, J(PH) 10.3, 7.3 Hz) and phenyl and C_6H_4 resonances between δ 7.9 and 6.1 in the ^{1}H NMR spectrum. The FAB mass spectrum of **7** had a molecular ion at m/z 1181, which, in conjunction with analytical, ^{1}H and ^{31}P NMR data, allowed the formulation of **7** as $Ru_5(\mu\text{-H})(\mu_4\text{-PPh})\{\mu_4\text{-}\eta^4\text{-CCPh}(C_6H_4)\}(\mu_3\text{-PPh})(CO)_{10}$. The ^{31}P NMR data confirmed the presence of two mutually *trans* phosphinidene groups with signals at δ 455.9 (d, J(PP) 78 Hz) and 480.4 (d, J(PP) 80 Hz) (on the basis of the observed couplings). In the ^{13}C NMR spectrum of **7**, the chemical shifts for C^α (δ 243.2) and C^β (δ 117.1) are similar to those found in ruthenium acetylide clusters [8,17]. This suggests that the

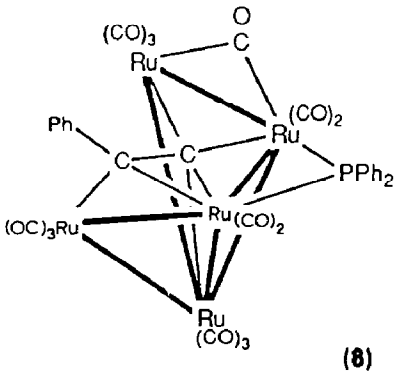

(8)

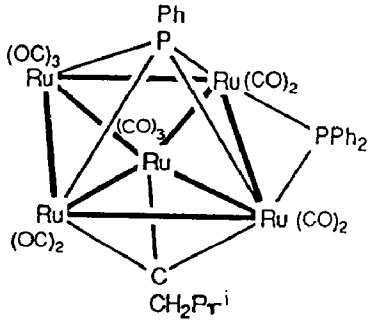

(9)

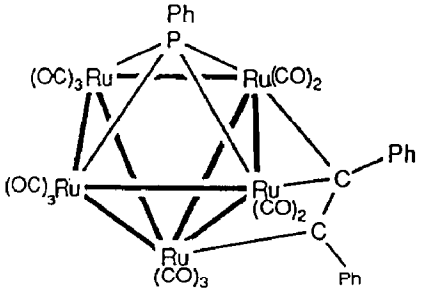

(10)

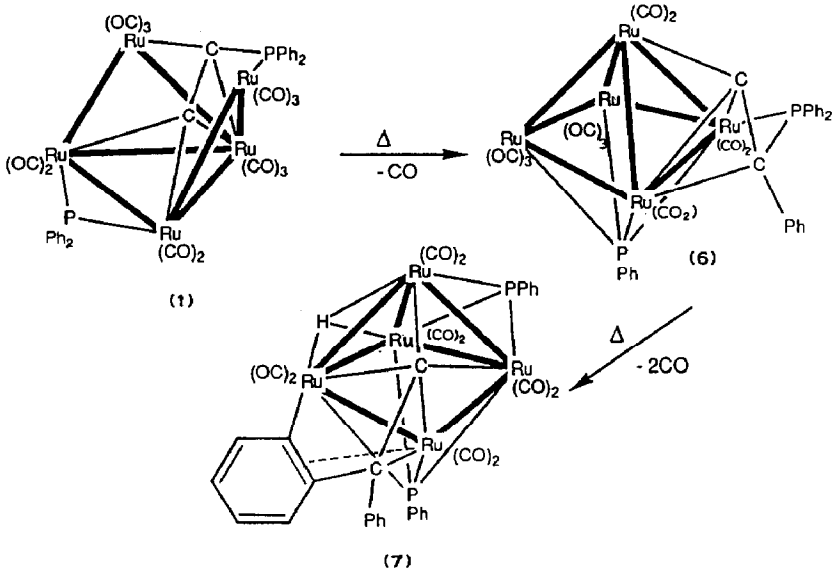

(1) (6) (7)

Scheme 2. Formation of **6** and **7** from **2**.

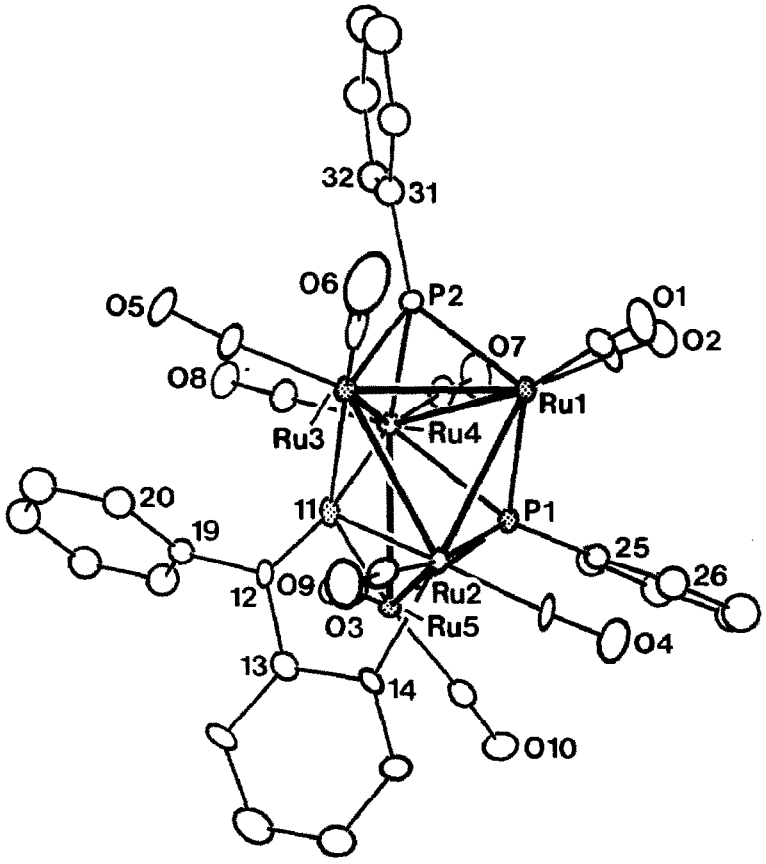

Fig. 4. ORTEP view of $Ru_5(\mu_3\text{-}H)(\mu_4\text{-}PPh)\{\mu_4\text{-}CCPh(C_6H_4)\}(\mu_3\text{-}PPh)(CO)_{10}$ (7) showing atom-labelling scheme. Atoms not otherwise indicated are carbons.

electronic differences between acetylide and vinylidene ligands on clusters are not large. Signals for seven different carbonyl environments were also observed (2 singlets, 4 doublets, 1 triplet) in the ^{13}C NMR spectrum at room temperature. On the basis of the observed C_i symmetry for 7, 10 carbonyl environments are expected, so it appears that either some signals are accidentally degenerate or limited carbonyl scrambling is occurring.

In complex 7 (Fig. 4), the five ruthenium atoms define a arrowhead framework as found previously in many Ru_5C clusters [19]. When the phosphorus and vinylidene C^{α} atoms (P(1), C(11)) are included, the $CPRu_5$ atom skeleton is a pentagonal bipyramid. A least-squares plane passes through P(1)Ru(5)C(11)Ru(3)Ru(1), the atoms which define the pentagonal plane (maximum deviations < 0.08 Å). Distortion from the typical butterfly arrangement is evident in the metal framework of 7, with Ru(1)–Ru(2) (3.065(1) Å) longer than Ru(2)–Ru(3) (2.895(1) Å). The μ_3-phosphinidene displays a reasonably symmetrical disposition about the Ru(4)Ru(1)Ru(3) face in 7, while the μ_4-phosphinidene is distorted towards the Ru(1)Ru(5) vector. The μ_4-carbon is also asymmetrically bonded to a Ru_4 face (Ru(2)–C(11) 2.14(1) Å, Ru(4)–C(11) 2.37(1) Å). Presumably, the bonding interactions of the allyl system with the metal core affect the disposition of C^{α}. The C=C bond length (1.41(3) Å) is comparable to those of other cluster-bound vinylidenes [14]. The vinylidene sub-

stituents are a phenyl and a metallated C_6H_4 group, the latter involved in an allylic interaction with Ru(5) (Ru(5)–C(12) 2.26(1) Å, Ru(5)–C(13) 2.33(1) Å, Ru(5)–C(14) 2.23(1) Å) and a σ-interaction with Ru(2) (Ru(2)–C(14) 2.14(1) Å).

Structure **2** can also be related to a pentagonal bipyramid, having a *nido* structure; however different atoms define the pentagonal plane: Ru(1)Ru(2)Ru(3) Ru(4) (**2**) (one vertex missing), and P(1)Ru(5)C(11)Ru(3)Ru(1) (**7**). The formation of these clusters may therefore be considered to demonstrate the interconversion between an open cluster (**2**), where the organic unit interacts with the surface, and a closed cluster (**7**), where the organic moiety is incorporated into the cluster.

Although no other intermediates were detected, it is probable that the conversion of **2** to **7** proceeds by stepwise loss of the three carbonyl groups accompanied by skeletal rearrangements. In **7**, the acetylide has been transformed, through phenyl migration (via P–C bond cleavage), into a vinylidene unit; this is coordinated via C^{β} and the metallated phenyl ring (C(12)C(13)C(14)) to Ru(5) and Ru(2). In the course of metallation, a hydrogen atom transfer to the cluster framework. Such a transfer has been noted previously in the formation of $Os_3(\mu\text{-H})\{\mu_3\text{-}(C_6H_4)PPh_2\}(CO)_8(PPh_3)$ [20]. The bond elongations Ru(1)–Ru(2) (3.065(1) Å), Ru(2)–Ru(3) (2.895(1) Å) ($Ru\text{–}Ru_{av.}$ 2.833 Å) [21] and coupling to two phosphinidene groups in the ^1H NMR hydride signal suggest that the hydride is μ_3-bonding the Ru(1)Ru(2)Ru(3) face. This is also supported by structural similarities with the complex $Ru_5(\mu_3\text{-H})(\mu_4\text{-PPh})_2(\mu_3\text{-PPh})(\mu\text{-PPh}_2)(CO)_{10}$ (**11**) [16] where the hydride was located on a similar face, and by the space-filling model of **7** (Fig. 5) where the

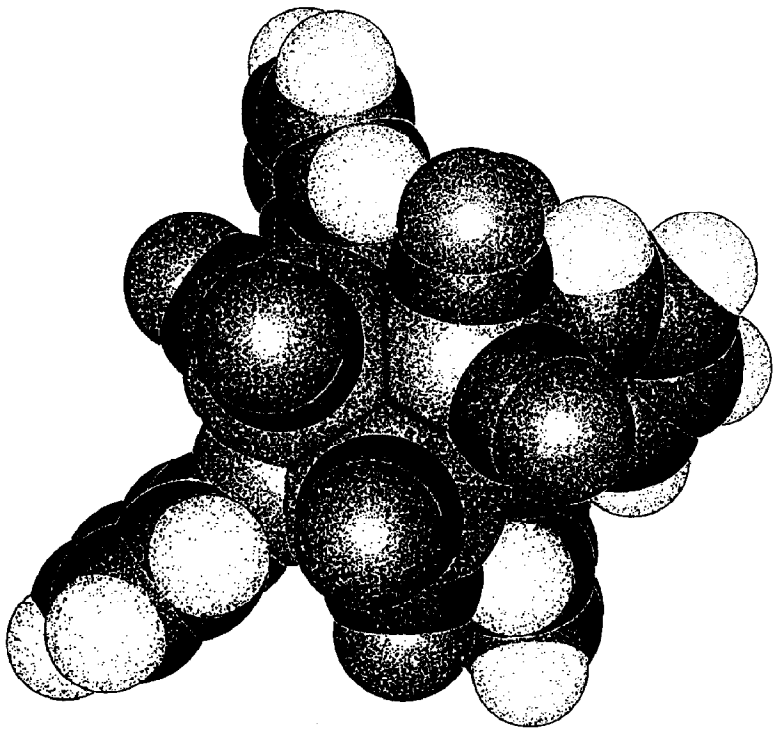

Fig. 5. JACKAL space-filling plot of **7**, showing Ru(1)Ru(2)Ru(3) face and cavity formed by CO groups thereon.

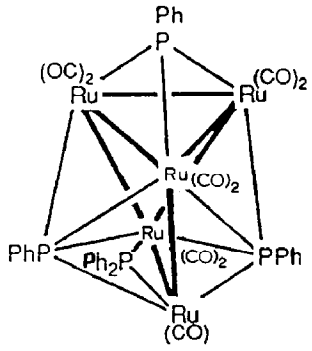

(11)

disposition of the carbonyl ligands on the Ru(1)Ru(2)Ru(3) face reveal a cavity in which the μ_3-H atom could reside.

When **7** was stirred for 24 h in MeOH, transformation to $Ru_5(\mu_4\text{-PPh})\{\mu_4\text{-}\eta^4\text{-CCPh}(C_6H_4)\}\{\mu\text{-PPh(OMe)}\}(CO)_{11}$ (**12**) occurred; this brown product was isolated in 38% yield after thin layer chromatography. In the proton NMR a doublet at δ 3.14 (J(PH) 14.2 Hz) indicated the presence of a Me group coupled to phosphorus; no metal-hydride ligands were present. The FAB mass spectrum confirmed that addition of MeO and CO had occurred, with a molecular ion at m/z 1238. Eight carbonyl resonances (5 singlets, 1 doublet, 2 multiplets) were observed in the ^{13}C NMR spectrum of **12** at room temperature. On the basis of the observed C_i symmetry for **12** (see Fig. 6), it appears that either some signals are accidentally degenerate or that limited carbonyl scrambling is occurring. The α- and β-carbon environments (δ 258.4, 107.7, respectively) are similar to those of **7**. A second brown band that was collected quickly converted into **12** (15 min for total conversion in CH_2Cl_2/cyclohexane solution, at 25 °C). The speed of the conversion precluded a detailed characterization of this band, but data from the FAB mass spectrum and low temperature ^1H and ^{31}P NMR spectra confirmed that this complex has the same formulation as **12**. This isomer is probably related to **12** by a structural transformation such as is shown in Scheme 3. The origin of the extra CO ligand in **12** has not been determined, but because of the large amount of decomposition observed in the reaction, it seems likely that intermolecular CO transfer is involved. The other eight minor bands and a large amount of intractable material on the base of the TLC plates were not isolated.

An X-ray crystal structure determination was carried out on **12**, and confirmed that addition of MeO to a PPh ligand had occurred to form the μ-phosphido group. The molecular structure is shown in Fig. 6 and bond distances and angles are listed in Table 3. Compounds **7** and **12** share a common metal core, the five ruthenium atoms defining a wingtip-bridged butterfly (or arrowhead) framework. When the phosphorus and C^{α} vinylidene carbon atoms (P(1), C(13)) are included in the atom skeleton of complex **12**, the geometry is again that of a pentagonal bipyramid with a least-squares plane passing through P(1)Ru(5)C(13)Ru(3)Ru(1) (maximum deviation < 0.13 Å). No appreciable bonding interaction was found between Ru(2) and Ru(4)

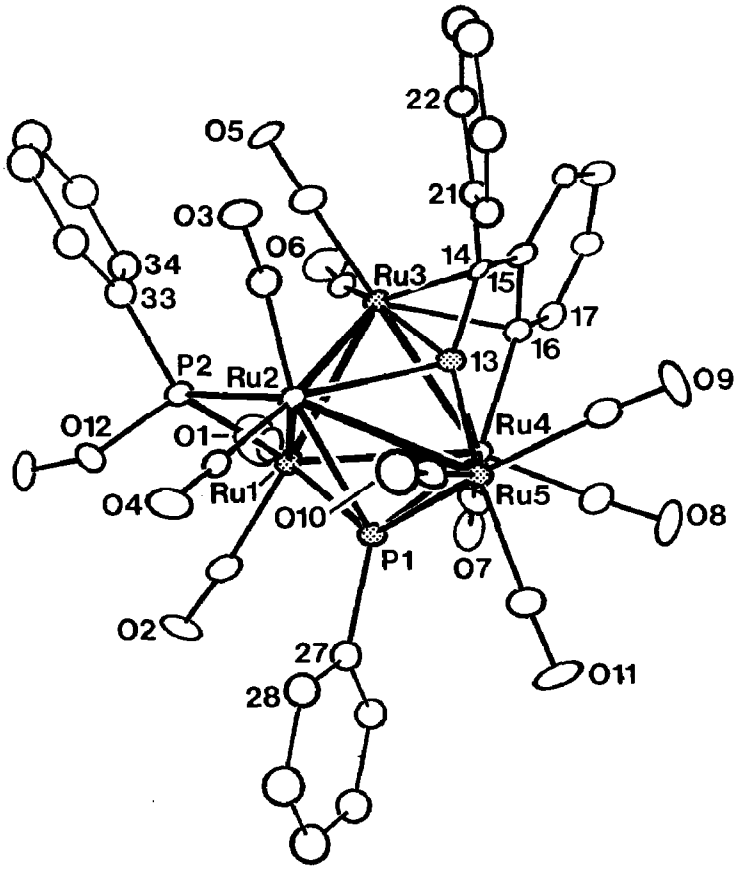

Fig. 6. ORTEP view of $Ru_5(\mu_4\text{-PPh})\{\mu_4\text{-CCPh}(C_6H_4)\}\{\mu\text{-PPh(OMe)}\}(CO)_{11}$ (**12**) showing atom-labelling scheme. Atoms not otherwise indicated are carbons.

in either complex (3.605(1) Å (**7**), 3.596(1) Å (**12**)), although in each case relatively small angles are subtended at the bridgehead atoms (Ru(2)Ru(5)Ru(4) 80.2(1)° (**7**), 76.9(1)° (**12**)) and the dihedrals at the hinge are also small (90.5° (**7**), 93.0° (**12**)).

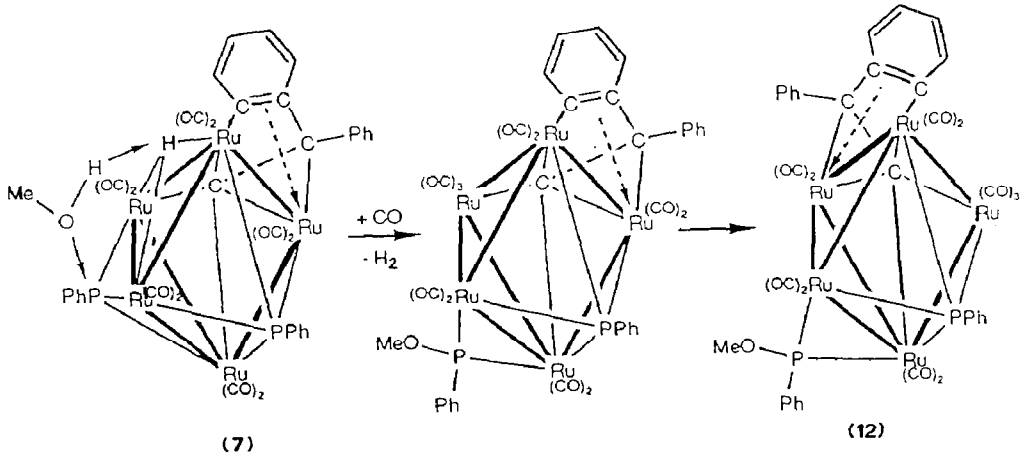

Scheme 3. Reaction of **7** with MeOH to form **12**.

Table 3

Selected bond lengths (Å) for **12**

Ru(1)–Ru(2)	2.811(2)	Ru(1)–Ru(3)	2.820(2)
Ru(1)–Ru(4)	2.929(2)	Ru(2)–Ru(3)	2.902(2)
Ru(2)–Ru(4)	3.596(2)	Ru(2)–Ru(5)	2.941(2)
Ru(3)–Ru(4)	2.752(2)	Ru(4)–Ru(5)	2.842(2)
Ru(1)–P(1)	2.394(4)	Ru(2)–P(1)	2.484(4)
Ru(4)–P(1)	2.370(4)	Ru(5)–P(1)	2.357(4)
Ru(1)–P(2)	2.225(5)	Ru(2)–P(2)	2.256(5)
Ru(2)–C(13)	2.41(2)	Ru(3)–C(13)	2.19(1)
Ru(4)–C(13)	2.18(2)	Ru(5)–C(13)	2.05(1)
Ru(3)–C(14)	2.21(1)	Ru(3)–C(15)	2.30(2)
Ru(3)–C(16)	2.29(2)	C(13)–C(14)	1.41(2)
C(14)–C(15)	1.51(2)		

These appear to be the first examples of M_5 clusters that are held together by both μ_4-vinylidene and μ_4-phosphinidene groups to form closo structures. In **12**, the effect of the phosphinidene and phosphido groups bridging Ru(1)–Ru(2) is to shorten this bond (2.840(1) Å (**7**), 2.811(2) Å (**12**), respectively); Ru(1)–Ru(4) (2.929(2) Å) and Ru(3)–Ru(4) (2.752(2) Å) are also shorter than in **7**. The difference in the latter two bond lengths in similar Ru_5C clusters is typically only 0.01 Å [19]. The distortion of the μ_4-phosphinidene in complex **12** is towards Ru(4)Ru(5).

The α-carbon is asymmetrically bonded to the Ru_4 face with Ru(4)–C(13) much shorter than Ru(2)–C(13) (2.18(2) Å, 2.41(2) Å, respectively). The C=C bond length (1.41(2) Å) is the same as that in **7** (1.41(3) Å). Complexes **7** and **12** are the first examples of clusters containing a μ_4-η^3 vinylidene without a hydrogen substituent on C^{β}. The switch of the allyl interaction from Ru(5) (**7**) to Ru(3) (**12**) occurs as a result of the new bonding requirements and the formation of the alkoxyphosphido group. The rearrangement shown in Scheme 3 is postulated because it assumes the smallest number of bonds broken/formed in the course of the reaction. The addition of methanol to the phosphinidene in **7** appears to be without precedent [22], and presumably occurs through nucleophilic attack by the methoxy group in conjunction with hydrogen transfer to the cluster, followed by loss of H_2.

The reaction between $Ru_3(CO)_{12}$ and $PHPh_2$ afforded the crystallographically characterised complex $Ru_5(\mu\text{-H})(\mu_4\text{-PPh})\{\mu\text{-PPh(OPr)}\}(CO)_{13}$ as a minor (1%) product. Its formation was ascribed to insertion of the carbonyl group of acrolein, present in trace amounts in the reaction solvent, with a P–H bond to give the propoxy groups [32].

^{31}P NMR studies on some Ru_4, Ru_5 and Au_2Ru_5 clusters

The ^{31}P NMR data gathered in the course of this work is presented in Table 4. Wherever the complexes containing phosphine, phosphite, phosphido and phosphinidene ligands have been crystallographically characterized, correlations between the ^{31}P NMR spectra and these structures have been made. A number of related compounds, which were not crystallographically characterized, are also listed in Table 4.

A recent review [23] has shown the usefulness of ^{31}P NMR chemical shift and coupling constant information in defining the stereochemistry of transition metal

Table 4

$^{31}P\{^1H\}$ NMR data for some Ru_4, Ru_5 and Au_2Ru_5 clusters [a]

Compound	C_2PPh_2 or C_2PhPPh_2	μ-PPh_2 μ-PPh(OMe)	μ_3-PPh	μ_4-PPh	$P(OEt)_3$	PPh_3 or PMe_2Ph	PPh_3 or $P(OEt)_3$
dppa	−31.0	–	–	–	–	–	–
2	38.1	310.6	–	–	–	–	–
3	–	0.1 (d, J = 100)	–	191.6 (d, J = 100)	–	–	–
4k	7.7	192.1	–	–	–	–	–
4t	10.5 (d, J = 123)	187.0 (d, J = 125)	–	–	–	–	–
5	–	131.9	–	–	–	–	–
6	−34.7	–	–	475.7	–	–	–
7	–	–	455.9 (d, J = 78)	480.4 (d, J = 80)	–	–	–
12	–	297.2 (d, J = 30)	–	326.1 (d, J = 30)	–	–	–
13a	44.2	292.9	–	–	140.8	–	–
13b	43.5 (m)	300.0 (m)	–	–	134.1 (2×d, J = 35,34)	–	–
13c	43.9	292.5	–	–	137.6	–	–
14	44.8 (d, J = 40)	277.3	–	–	142.8	–	137.1 (d, J = 40)
15	39.2	269.6	–	–	–	23.7	1.5
16	41.0	281.3	–	–	–	–	–
17	–	203.7 (m)	–	451.5	–	–	–
18	−6.0	213.8	–	–	–	74.9	62.6
19	−6.3	214.3	–	–	186.3	71.3	–
20	0.4	202.5	–	–	185.7	71.0	130.2
21	1.3	203.4	–	–	129.2	74.7	62.3
22	44.5	194.8	–	–	–	–	–
23	40.3	194.3	–	–	–	–	–
24	64.1	236.6	–	–	–	–	–
25	49.5	189.1	–	–	–	60.4	–

[a] All spectra were recorded in CH_2Cl_2; peak positions are relative to ext. 85% H_3PO_4. Compounds not otherwise identified in this paper are: isomers **a**, **b** and **c** of $Ru_5(\mu_5\text{-}C_2PPh_2)(\mu\text{-}PPh_2)(CO)_{12}\{P(OEt)_3\}$ (**13**); $Ru_5(\mu_5\text{-}C_2PPh_2)(\mu\text{-}PPh_2)(CO)_{11}\{P(OEt)_3\}_2$ (**14**); $Ru_5(\mu_5\text{-}C_2PPh_2)(\mu\text{-}PPh_2)(CO)_{11}(PMe_2Ph)_2$ (**15**); $Ru_5(\mu_5\text{-}C_2PPh_2)(\mu\text{-}PPh_2)(CO)_{12}(PPh_3)$ (**16**); $Ru_5(\mu_4\text{-}PPh)(\mu\text{-}PhC_2Ph)(\mu\text{-}PPh_2)_2(CO)_{10}$ (**17**); $Au_2Ru_5(\mu_5\text{-}C_2PPh_2)(\mu\text{-}PPh_2)(CO)_{12}(PPh_3)_2$ (**18**); $Au_2Ru_5(\mu_5\text{-}C_2PPh_2)(\mu\text{-}PPh_2)(CO)_{12}(PPh_3)\{P(OEt)_3\}$ (**19**); $Au_2Ru_5(\mu_5\text{-}C_2PPh_2)(\mu\text{-}PPh_2)(CO)_{11}(PPh_3)\{P(OEt)_3\}_2$ (**20**); $Au_2Ru_5(\mu_5\text{-}C_2PPh_2)(\mu\text{-}PPh_2)(CO)_{11}(PPh_3)_2\{P(OEt)_3\}$ (**21**); $Ru_5(\mu\text{-}H)(\mu_5\text{-}C_2PPh_2)(\mu\text{-}PPh_2)(\mu\text{-}Cl)(CO)_{12}$ (**22**); $Ru_5(\mu\text{-}H)(\mu_5\text{-}C_2PPh_2)(\mu\text{-}PPh_2)(\mu\text{-}Br)(CO)_{13}$ (**23**); $Ru_5(\mu\text{-}H)(\mu_5\text{-}C_2PPh_2)(\mu_3\text{-}I)(\mu\text{-}PPh_2)(CO)_{12}$ (**24**); $AuRu_5(\mu_5\text{-}C_2PPh_2)(\mu\text{-}PPh_2)(\mu\text{-}Cl)(CO)_{13}(PPh_3)$ (**25**).

complexes which contain phosphido and phosphinidene ligands. Huttner et al. [24] have recorded a series of chemical shifts for various $Ru_5(\mu_4\text{-}PR_3)(CO)_{15}$ (R = Ph, Et, Me, CH_2Ph) clusters, and a small number of other Ru_5 clusters were also mentioned in the review article [23]. The work presented here extends considerably the amount of information pertaining to pentanuclear ruthenium clusters.

Phosphinidene ligands. Phosphinidene ligands, in both the μ_4 and μ_3 modes of coordination, were found in several of these complexes. Two structural types containing μ_4-PPh groups have been found for the Ru_5 clusters: the first was the

arrowhead core, which has an open Ru_4 face capped by a phosphinidene ligand. Complexes **7** and **12** have this geometry and the chemical shifts for the phosphinidenes were found at δ 480.4 and 326.1, respectively. (The assignment of the signal for **7** is somewhat arbitrary as there is also a μ_3-phosphinidene present at δ 455.9.) Both phosphinidenes in complex **7** are coupled (J_{av} 79 Hz). Similar coupling was found between the phosphido and phosphinidene ligands in **12**, these groups being attached to the Ru(1)–Ru(4) bond as is the μ_3-PPh. The second structural type is that based on a square pyramid, examples being **6** and **17**. The chemical shifts for the phosphinidene ligands in these clusters were at δ 475.7 and 451.5, respectively. No coupling was observed between the phosphino-vinylidene and phosphinidene ligands in **6**. The phosphinidene ligand in **3** had a signal at δ 191.6 showing P–P coupling (100 Hz) to the phosphino-alkyne ligand. This high field shift has a precedent in the signal found at δ −34 for one of the phosphinidene ligands in $Ru_4(\mu_4\text{-PPh})_2(\mu\text{-PPhH})_2(CO)_8$ [25].

Bridging phosphido ligands. The chemical shift for the phosphido bridge in **2** is at particularly low field (δ 310.6). Similar shifts (δ 277.3–292.9) were found for the swallow-geometry, phosphite-substituted clusters **13a**, **13c** and **14**. No phosphorus coupling was observed between the $P(OEt)_3$ ligand in **13c** and the phosphido ligand; this is not surprising as the phosphite is attached in a *cis* fashion to the phosphido-bound ruthenium (P(2)Ru(3)P(3) 102.3(1)°). The μ-PPh(OMe) ligand in **12** showed had a signal at δ 297.2. For the square pyramidal cluster **17**, the phosphido signals appeared at δ 203.7. The third pentanuclear framework to have been examined was that of the scorpion geometry, of which **4k**, **4t**, **23** and **24** are examples. The chemical shifts for the phosphido groups in these complexes are δ 192.1, 187.0, 194.3 and 236.6, respectively. There was a large P–P coupling constant ($J_{av.}$ 124 Hz) between the phosphido and phosphino-acetylide ligands in **4t**, as these ligands are in a *trans* arrangement (RuPRu 141.0(1)°). A signal was found at δ 131.9 for the two equivalent phosphido groups bridging the Ru_3 triangles in **5**. The heptanuclear cluster **21** showed a higher field shift for the phosphido group (δ 203.4) than did **13a** (which is the most closely related Ru_5 complex).

Phosphine and phosphite ligands. The phosphino-acetylide ligands in the penta-ruthenium clusters showed chemical shifts in the range δ 38.1–44.8 for the swallow clusters and δ 7.7–64.1 for the scorpion clusters. Coordination and rearrangement of the dppa ligand has moved the chemical shift of the phosphorus to a lower field than that of the free ligand (δ −31.0). The Au_2Ru_5 clusters had signals for the C_2PPh_2 ligand between δ −6.3 and 1.3, the effect of adding the digold unit to **2** being to shield the phosphorus nuclei. Complex **14** showed P–P coupling (40 Hz) between the phosphino-acetylide and the $P(OEt)_3$ ligand on Ru(1). As mentioned above, a large P–P coupling constant (100 Hz) was found between the phosphino-alkyne and phosphinidene ligands in the tetranuclear cluster **3**; the chemical shift of the phosphino-alkyne was δ 0.1. The novel phosphino-vinylidene ligand present in **26** has a chemical shift of δ −34.7. The substituted derivatives **13a**, **13c**, **14** and **21** had chemical shifts for the triethylphosphite ligands in the normal region for such ligands δ 129.2–140.8, while the triphenylphosphine ligands in complex **21** had signals at δ 62.3 and 74.7.

The utility of ^{31}P NMR studies in characterizing multinuclear clusters relies on a sufficiently large body of data having been correlated with the known structural types. When such information becomes available combination of analytical results,

FAB MS, ^{1}H NMR, ^{13}C NMR and ^{31}P NMR data may provide quite detailed information on the stereochemistry of new complexes without recourse to X-ray studies. In favourable circumstances, the time required to obtain an X-ray crystal structure is likely to be shorter than that required for an analytical and spectroscopic characterization, and the result more certain. In particular, for complexes that are likely to have new structural geometries, the ^{31}P NMR results must be treated cautiously, as the chemical shift regions of the various phosphorus ligands examined have been shown to overlap and X-ray studies become essential.

Experimental

General conditions

All reactions were carried out under dry, oxygen-free nitrogen by standard Schlenk techniques. Solvents were dried and distilled before use. Elemental analyses were by the Canadian Microanalytical Service, New Westminster, B.C., Canada V3M 1S3.

Instruments: Perkin Elmer 683 double beam, NaCl optics (IR); Bruker WP80 (NMR; ^{1}H, at 80 MHz, ^{13}C, at 20.1 MHz) or CXP300 (^{1}H, at 300.13 MHz, ^{13}C, at 75.47 MHz, ^{31}P, at 121.49 MHz); VG ZAB 2HF (FAB MS, using 3-nitrobenzyl alcohol as matrix, exciting gas Ar, FAB gun voltage 7.5 kV, current 1 mA, accelerating potential 8 kV). Peaks are recorded as: m/z, relative intensity, assignment. TLC was carried out on glass plates (20×20 cm) coated with silica gel (Merck 60 GF254, 0.5 mm thick).

Synthesis

A large scale preparation of $Ru_5(\mu_5\text{-}\eta^2,P\text{-}C_2PPh_2)(\mu\text{-}PPh_2)(CO)_{13}$ (2)

Ten drops of sodium diphenyl ketyl (Na/bpk) solution (approx. 0.1 *M*) [26] were added to a degassed solution of $Ru_3(CO)_{12}$ (1.0 g, 1.56 mmol, finely ground) and dppa (310 mg, 0.79 mmol) in thf (90 ml). A N_2 stream was used to remove evolved CO. After 15 min another six drops of Na/bpk solution were added. Spot TLC analysis (petroleum spirit/CH_2Cl_2 4/1) of the deep orange solution indicated the presence of a trace amount of unchanged $Ru_3(CO)_{12}$ (R_f 0.77), two minor orange-red bands and the major orange product (R_f 0.57) $\{Ru_3(CO)_{11}\}_2(\mu\text{-dppa})$. The solvent was then removed under vacuum, the residue extracted with toluene (50 ml) and filtered through Celite into a two-necked flask (100 ml). Nitrogen was passed through the solution using a glass sinter, and the reaction heated to between 88 and 92°C for 1.5 h. The dark brown solution was monitored by TLC and IR for the disappearance of $\{Ru_3(CO)_{11}\}_2(\mu\text{-dppa})$. After cooling to −15°C for 15 h, the yellow precipitate of $Ru_3(CO)_{12}$ (150 mg, 0.23 mmol, 15%) was filtered off, washed with cold toluene (−15°C, 2×5 ml) and the filtrates evaporated to dryness. The residue was extracted with CH_2Cl_2 (20 ml), and MeOH (5 ml) was then added. Following volume reduction to 7 ml the solution was layered with MeOH (20 ml) and cooled to −15°C (3 h). This gave a first crop of dark brown crystalline $Ru_5(\mu_5\text{-}\eta^2\text{-}P\text{-}C_2PPh_2)(\mu\text{-}PPh_2)(CO)_{13}$ (2) (600 mg). The process of crystallization was repeated to give a further crop of 2 (210 mg), for a total yield of 2 of 810 mg (0,64 mmol, 82%). These crystallizations had to be performed carefully and reasona-

bly quickly to avoid co-crystallization of $Ru_4(\mu_4\text{-PPh})\{\mu_4\text{-}\eta^2,P\text{-}PhC_2PPh_2\}(\mu\text{-}CO)_2(CO)_8$ (**3**) (orange crystals). Although these complexes could be separated by TLC it was not possible on this scale to achieve reasonable separations by column chromatography on Florisil or silica.

New spectroscopic data for $Ru_5(\mu_5\text{-}\eta^2,P\text{-}C_2PPh_2)(\mu\text{-}PPh_2)(CO)_{13}$ *(2).* FAB MS: 1265, $[M]^+$; ions formed by stepwise loss of 13 CO groups. (After prolonged periods in the FAB beam peaks corresponding to the carbonylation isomers $Ru_5(\mu_5\text{-}\eta^2,P\text{-}C_2PPh_2)(\mu\text{-}PPh_2)(CO)_{15}$ (**4k** and **4t**) were observed at *m/z* 1321, $[M + 2CO]^+$; 1293, $[M + CO]^+$.) $^{13}C\{^1H\}$ NMR ($CDCl_3$): δ 239.0 (d, *J*(PC) 23 Hz, C^α); 202.5 (s), 201.5 (s), 199.2 (s), 198.9 (d, *J*(PC) 4 Hz), 197.7 (s), 194.5 (s), 194.1 (d, *J*(PC) 3 Hz), 193.9 (d, *J*(PC) 3 Hz), 192.5 (s) (Ru–CO); 143.5–128.4 (m, Ph); 108.8 (d, *J*(PC) 22 Hz, C^β). Electrochemistry (CH_2Cl_2): Differential pulse E_p^{red} −0.76 V; CV $E_{1/2}^{red}$ −0.78 V, E_{pc}^{red} −0.88 V, E_{pa}^{red} −0.67 V; this reduction process is quasi-reversible and is not diffusion controlled.

The supernatant liquid from the above synthesis was evaporated to dryness to give a brown residue. This residue was converted into $Ru_5(\mu\text{-H})(\mu_4\text{-PPh})\{\mu_4\text{-}\eta^4\text{-}CCPh(C_6H_4)\}(\mu_3\text{-PPh})(CO)_{10}$ (**7**) by the following procedure: the residue was first dissolved in CH_2Cl_2 and then supported on Florisil; the Florisil was then extracted with petroleum spirit/CH_2Cl_2 (1/1) and the solvent removed under vacuum (to remove all traces of MeOH). The resulting complex was then pyrolyzed in toluene and the product worked up as for the synthesis of **7** from **2** (see below).

The two minor products observed in the ETC reaction of $Ru_3(CO)_{12}$ with dppa were purified by preparative TLC (petroleum spirit/CH_2Cl_2 4/1). An orange compound (R_f 0.28) was formulated as $Ru_5(CO)_{13}$(dppa*). IR (cyclohexane): ν(CO) 2095m, 2074w, 2056(sh), 2044s, 2025(sh), 2013s cm^{-1}. FAB MS: 1265, $[M]^+$; ions formed by stepwise loss of two CO groups. The second, red, compound (R_f 0.45) was formulated as $Ru_6(Ph)(CO)_{16}$(dppa*). IR (cyclohexane): ν(CO) 2092(sh), 2085m, 2057s, 2048(sh), 2024(sh), 2017s, 1989(sh), 1967(sh) cm^{-1}. FAB MS 1526, $[M]^+$; ions formed by sequential loss of two CO groups.

Pyrolysis of $\{Ru_3(CO)_{11}\}_2(\mu\text{-dppa})$ *under different conditions*

(a) The product from $Ru_3(CO)_{12}$ (1 g, 1.56 mmol) and dppa (308 mg, 0.78 mmol) was dissolved in toluene (50 ml) and the solution kept under a N_2 blanket for 4 h at 90 °C. After removal of $Ru_3(CO)_{12}$ (142 mg, 0.22 mmol, 14%) by cooling (−15 °C), further crystallization (CH_2Cl_2/MeOH) gave a crop of **2** (510 mg, 0.40 mmol, 52%). The residue was purified by TLC (petroleum spirit/CH_2Cl_2 4/1); five bands were collected, the first four being identified (IR, FAB MS) as: (1) R_f 0.77, yellow, $Ru_3(CO)_{12}$; (2) R_f 0.57, orange, $\{Ru_3(CO)_{11}\}_2(\mu\text{-dppa})$; (3) R_f 0.52, brown, **2**; (4) R_f 0.50, yellow, $Ru_4(\mu_4\text{-}\eta^2\text{-}C_2)(\mu\text{-}PPh_2)_2(CO)_{12}$ (**5**). The solid recovered from the fifth band (R_f 0.48, orange) was fractionally crystallized (CH_2Cl_2/petroleum spirit) and the first crop of fine orange crystals identified as $Ru_4(\mu_4\text{-PPh})\{\mu_4\text{-}\eta^2,P\text{-}PhC_2PPh_2\}(\mu\text{-}CO)_2(CO)_8 \cdot 0.5CH_2Cl_2$ (**3**) (15 mg, 0.013 mmol, 2%), m.p. 175–176 °C (colour change at 160–163 °C). Anal. Found: C, 39.24; H, 1.96; M_r 1079 (mass spectrometry, $[M + H]^+ = 1080$). $C_{36}H_{20}O_{10}P_2Ru_4 \cdot 0.5CH_2Cl_2$ calcd.: C, 39.10; H, 1.89%. M_r 1079 (unsolvated). IR (cyclohexane): ν(CO) 2061w, 2030vs, 2008m, 2001w, 1982w, 1964w, 1878vw, 1851w cm^{-1}. ^1H NMR ($CDCl_3$): δ 7.7–7.2 (m, 20H, Ph); 5.30 (s, 1H, CH_2Cl_2). FAB MS: 1080, $[M]^+$; ions formed by stepwise loss of 10 CO groups. Slow evaporation of the supernatant solution gave a further

batch of orange crystals of $Ru_5(\mu_5\text{-}\eta^2,P\text{-}C_2PPh_2)(\mu\text{-}PPh_2)(CO)_{15}$ (**4t**) (22 mg, 0.016 mmol, 2%), identified by IR and spot TLC comparison with an authentic sample [4a].

New spectroscopic data for $Ru_5(\mu_5\text{-}\eta^2,P\text{-}C_2PPh_2)(\mu\text{-}PPh_2)(CO)_{15}$. FAB MS (**4t**): 1321, $[M]^+$; ions formed by stepwise loss of 15 CO groups. FAB MS (**4k**): 1321 $[M]^+$; fragmentation pattern identical with that of **4t**.

(b) A solution of $\{Ru_3(CO)_{11}\}_2(\mu\text{-dppa})$ (450 mg, 0.28 mmol) in toluene (50 ml) was refluxed for 90 min (under a N_2 blanket), and cooled; the $Ru_3(CO)_{12}$ side-product was removed by crystallization (−15 °C). Of the large number of products (8) isolated by preparative TLC (petroleum spirit/CH_2Cl_2 4/1), the major one was **2** (R_f 0.45). The product from a green band (R_f 0.53) was identified (IR, FAB MS) as $Ru_5(\mu_3\text{-H})(\mu_4\text{-PPh})\{\mu_4\text{-}\eta^4\text{-CCPh}(C_6H_4)\}(\mu_3\text{-PPh})(CO)_{10}$ (**7**). Fractional crystallization of the material from brown band (R_f 0.42) first gave a batch of orange crystals (CH_2Cl_2/petroleum spirit, −15 °C) which were identified (IR, FAB MS) as **3**. Following volume reduction and cooling of the supernatant, brown crystals of $Ru_5(\mu_4\text{-PPh})\{\mu_3\text{-}\eta^2,P\text{-CCPh}(PPh_2)\}(CO)_{12}$ (**6**), (identified by IR, FAB MS) were separated from an orange powder. The orange powder was assigned the formulation $Ru_8(CO)_{17}(dppa^*)$ from FAB MS data (m/z 1681, $[M]^+$). The last product may also be obtained by heating a mixture of **7** and $Ru_3(CO)_{12}$ in n-octane. Unfortunately, because of the low yields of this complex it was not possible to grow single crystals suitable for an X-ray study. Another complex of the formulation $Ru_5(CO)_{13}(dppa^*)$ was also isolated in the initial TLC separation (orange, R_f 0.38, 4 mg); this had the following properties: IR (cyclohexane): ν(CO) 2088m, 2081w, 2068s, 2044vs, 2038(sh), 2020vs, 2011(sh), 2002s(sh), 1990m, 1978(sh), 1963m cm^{-1}. FAB MS: 1265, $[M]^+$; ions formed by sequential loss of 13 CO groups.

Synthesis of $Ru_4(\mu_4\text{-}\eta^2\text{-}C_2)(\mu\text{-}PPh_2)_2(CO)_{12}$ *(5)*

A solution of compound **1** (100 mg, 0.079 mmol) in benzene (30 ml) was placed under 22 atm of CO and then heated at 105 °C for 21 h. After cooling, the solvent was removed from the yellow solution under reduced pressure and the residue chromatographed (TLC: petroleum spirit/CH_2Cl_2 4/1). Most of the mixture remained on the base-line. The product from yellow band (R_f 0.8) was identified (IR, spot TLC) as $Ru_3(CO)_{12}$ (11 mg, 0.017 mmol, 22%) and a minor yellow band (R_f 0.52) crystallized (CH_2Cl_2/petroleum spirit) as yellow cubes of $Ru_4(\mu_4\text{-}\eta^2\text{-}C_2)(\mu\text{-}PPh_2)_2(CO)_{12}$ (**5**) (10 mg, 0.0088 mmol, 11%) [4b], m.p. 158–160 °C (dec.), identified by comparison with an authentic sample (IR, unit cell dimensions).

New spectroscopic data for $Ru_4(\mu_4\text{-}\eta^2\text{-}C_2)(\mu\text{-}PPh_2)_2(CO)_{12}$ *(5).* m.p. 158–160 °C (dec.). ^1H NMR (C_6D_6): δ 7.2–6.2 (m, Ph). $^{13}C\{^1H\}$ NMR ($CDCl_3$): δ 198.0 (m), 196.6(m), 194.3(m) (Ru–CO); 141.1 (d, J(PC) 37 Hz, C_2; 133.2–128.4 (m, Ph). FAB MS: 1137, $[M]^+$; ions formed by stepwise loss of 12 CO groups.

Thermolysis of $Ru_5(\mu_5\text{-}\eta^2,P\text{-}C_2PPh_2)(\mu\text{-}PPh_2)(CO)_{13}$ *(2)*

Synthesis of $Ru_5(\mu_4\text{-PPh})\{\mu_3\text{-}\eta^2,P\text{-CCPh(PPh)}\}(CO)_{12}$ *(6)*

A solution of **2** (250 mg, 0.20 mmol) in toluene (60 ml) was heated (oil bath, 170 °C) for 2.5 h with N_2 passing through. The solvent was removed under reduced pressure and the residue separated by column chromatography on Florisil. A major green band was removed (petroleum spirit) and identified (IR, FAB MS) as **7** (110

mg, 0.093 mmol, 47%). The next, brown, band (eluent: petroleum spirit/CH_2Cl_2 2/1) was collected, and subjected to TLC (petroleum spirit/CH_2Cl_2 4/1). A small amount of **7** was recovered (R_f 0.68, green band), followed by a major brown band (*Rf* 0.58), the product from which was crystallized (CH_2Cl_2/MeOH) to give dark brown crystals of $Ru_5(\mu_4\text{-PPh})\{\mu_3\text{-}\eta^2,P\text{-CCPh}(PPh_2)\}(CO)_{12}$ (**6**) (54 mg, 0.044 mmol, 22%), m.p. 205–207 °C. Anal. Found: C, 36.81; H, < 2. M_r 1236 (mass spectrometry). $C_{38}H_{20}O_{12}P_2Ru_5$ calcd.: C, 36.93; H, 1.63%. M_r 1236. IR (cyclohexane): ν(CO) 2072m, 2041s, 2025s, 2008s, 1985w, 1968w, 1953w cm^{-1}. ^1H NMR (C_6D_6): δ 7.9–6.8 (m, Ph). $^{13}C\{^1H\}$ NMR ($CDCl_3$, $Cr(acac)_3$): δ 202.6 (m), 197.0(m), 192.6(s), 192.3(s) (Ru–CO); 148.8 (d, J(PC) 15 Hz, C^α); 133.6–127.8 (m, Ph); 109.2 (m, C^β), FAB MS: 1236, $[M]^+$; ions formed by stepwise loss of 10 CO groups.

Synthesis of $Ru_5(\mu_3\text{-H})(\mu_4\text{-PPh})\{\mu_4\text{-}\eta^4\text{-CCPh}(C_6H_4)\}(\mu_3\text{-PPh})(CO)_{10}$ *(7)*

(a) Conversion of **2** *to* **7**. A solution of **2** (200 mg, 0.16 mmol) in toluene (50 ml) was refluxed for 2 h (oil bath, 155 °C), with N_2 flowing through. During this time the mixture became green, and monitoring by spot TLC confirmed the disappearance of the starting material. The solvent was removed under vacuum and the residue purified by TLC (petroleum spirit/CH_2Cl_2 4/1). The solid isolated from a major green band (R_f 0.53) was crystallized (hexane/cyclohexane) by slow evaporation as dark green-black crystals of $Ru_5(\mu_3\text{-H})(\mu_4\text{-PPh})\{\mu_4\text{-}\eta^4\text{-CCPh}(C_6H_4)\}(\mu_3\text{-PPh})(CO)_{10}\cdot 0.5C_6H_{14}$ (**7**) (122 mg, 0.10 mmol, 65%), m.p. 170–172 °C. Anal. Found: C, 38.20; H, 2.22. M_r 1180 (mass spectrometry), 1181 = $[M+H]^+$. $C_{36}H_{20}O_{10}P_2Ru_5\cdot 0.5C_6H_{14}$ calcd.: C, 38.30; H, 2.33. M_r 1180 (unsolvated). IR (cyclohexane): ν(CO) 2056vw, 2030vs, 2024(sh), 2016s, 2012(sh), 1982m, 1977(sh), 1966m cm^{-1}. ^1H NMR (C_6D_6): δ 7.9–6.1 (m, 19 H, Ph + C_6H_4); 0.99 (m, 4H, CH_2, hexane); 0.58 (m, 3H, CH_3, hexane); −15.38 (dd, J_{PH} = 10.3, 7.3 Hz, 1H, RuH). $^{13}C\{^1H\}$ NMR (CH_2Cl_2): δ 243.2 (d, J(PC) 11 Hz, C^α); 199.0 (s), 198.1 (s), 197.5 (d, J(PC) 13 Hz), 193.7 (t, J(PC) 31 Hz), 192.6 (d, J(PC) 29 Hz), 191.4 (d, J(PC) 27 Hz), 190.1(d, J(PC) 31 Hz) (Ru–CO); 149.3–124.6 (m, Ph); 117.1 (s, C_β). FAB MS: 1181, $[M]^+$; ions formed by sequential loss of 10 CO groups. Two minor bands were also observed; of these the brown band (R_f 0.42) contained **6** (IR, FAB MS). For preparative purposes it was found that a slightly longer reaction duration (2.5 h), and column chromatography (Florisil, eluent petroleum spirit) allowed the isolation of **7** in higher yields. Due to the high solubility of this compound in hydrocarbon solvents the product was generally evaporated to dryness under vacuum to obtain a sample suitable for further reactions.

(b) Conversion of **6** *to* **7**. A solution of complex **6** (9 mg, 0.007 mmol) in toluene (15 ml) was refluxed for 4.25 h with N_2 flowing through. After cooling, the solvent was removed and the residue chromatographed (TLC: petroleum spirit/CH_2Cl_2 4/1). A major green band (R_f 0.50) was identified (IR, spot TLC) as $Ru_5(\mu_3\text{-H})(\mu_4\text{-PPh})\{\mu_4\text{-}\eta^4\text{-CCPh}(C_6H_4)\}(\mu_3\text{-PPh})(CO)_{10}$ (**7**) (6 mg, 0.005 mmol, 73%) and a minor brown band (R_f 0.38) was collected and the solid isolated from it identified (IR, spot TLC) as unchanged **6** (1 mg, 0.008 mmol, 11%); two trace bands and a brown base-line were also observed.

Synthesis of $Ru_5(\mu_4\text{-PPh})\{\mu_4\text{-}\eta^4\text{-CCPh}(C_6H_4)\}\{\mu\text{-PPh(OMe)}\}(CO)_{11}$ *(12)*

Methanol (15 ml) was added to complex **7** (100 mg, 0.085 mmol), and the mixture was stirred vigorously for 24 h. The solvent was removed from the brown solution

under reduced pressure and the residue purified by TLC (petroleum spirit/CH_2Cl_2 8/3). A major brown band (R_f 0.50) was collected and the recovered solid was recrystallized (CH_2Cl_2/MeOH) to give dark brown rhomboids of $Ru_5(\mu_4\text{-PPh})\{\mu_4\text{-}\eta^4\text{-CCPh}(C_6H_4)\}\{\mu\text{-PPh(OMe)}\}(CO)_{11}$ (**12**) (40 mg, 0.032 mmol, 38%), m.p. 115–117 °C. Anal. Found: C, 36.32; H, 2.04. M_r 1238 (mass spectrometry). $C_{38}H_{22}O_{12}P_2Ru_5$ calcd.: C, 36.87; H, 1.79%. M_r 1238. IR (cyclohexane): ν(CO) 2081m, 2038s, 2033(sh), 2021s, 2001s, 1995(sh), 1990m, 1982vw, 1973w, 1969(sh), 1952w cm^{-1}. ^1H NMR (CD_2Cl_2): δ 8.4–6.9 (m, 19H, Ph + C_6H_4); 3.14 (d, J(PH) 14.2 Hz, 3H, OMe). $^{13}C\{^1H\}$ NMR (CH_2Cl_2): δ 258.4 (d, J(PC) 14 Hz, C^α); 210.3 (d, J(PC) 36 Hz), 206.9 (s), 202.0 (s), 200.4 (s), 198.0 (s), 193.7 (m), 192.8 (m), 189.2 (s) (Ru–CO); 146.3–123.1 (m, Ph); 107.7 (s, C^β); OMe resonance probably under CH_2Cl_2 peak [27]. FAB MS: 1238, $[M]^+$; ions formed by stepwise loss of 10 CO groups. Of the ten other minor/trace bands only a brown band (R_f 0.15) was collected. This was precipitated quickly (CH_2Cl_2/petroleum spirit) as a brown powder which was unstable in solution. In cyclohexane conversion of this product to **12** was complete (IR, spot TLC) within 15 min. The brown powder also has the formulation $Ru_5(\mu_4\text{-PPh})\{\text{CCPh}(C_6H_4)\}\{\mu\text{-PPh(OMe)}\}(CO)_{11}$ (15 mg, 0.012 mmol, 14%). IR (cyclohexane): ν(CO) 2050w, 2025s, 2017s, 1980w, 1962w cm^{-1}. ^1H NMR (acetone-d_6, 240 K); δ 8.2–6.9 (m, Ph); 3.17 (d, J(PH) 14.4 hz, OMe). $^{31}P\{^1H\}$ NMR (acetone-d_6, 240 K): δ 305.5 d, J(PP) 26 Hz, μ_4-PPh); 299.2 (d, J(PP) 26 Hz, μ-P(OMe)Ph). FAB MS: 1239, $[M]^+$; ions formed by stepwise loss of 10 CO groups.

Table 5

Crystal and intensity collection data for **3**, **6**, **7** and **12**

	3	**6**	**7**	**12**
Formula	$C_{37}H_{24}O_{11}P_2Ru_4$	$C_{38}H_{20}O_{12}P_2Ru_5$	$C_{36}H_{20}O_{10}P_2Ru_5$	$C_{40}H_{32}O_{15}P_2Ru_5$
M_r	1110.8	1235.8	1179.8	1317.9
Cryst. system	monoclinic	monoclinic	monoclinic	monoclinic
Space group	$P2_1/c$ (C_{2h}^5, No. 14)	$P2_1/n$ (variant C_{2h}^5, No. 14)	$P2_1/c$ (C_{2h}^5, No. 14)	$P2_1/c$ (C_{2h}^5, No. 14)
a, Å	10.918(4)	17.981(5)	12.972(5)	20.556(2)
b, Å	17.766(3)	13.07(1)	11.169(1)	10.698(2)
c, Å	20.229(13)	18.00(2)	29.629(8)	21.536(3)
β, deg	103.98(3)	97.0(1)	97.62(2)	98.62(2)
U, Å^3	3807.6	4199	4254.9	4682.4
Z	4	4	4	4
D_{calcd}, g cm^{-3}	1.938	1.955	1.842	1.870
μ, cm^{-1}	16.35	18.26	17.97	16.45
max/min transmission factors	0.798; 0.515	0.734; 0.628	0.740; 0.431	0.806; 0.687
F(000)	2160	2376	2264	2568
θ range, deg	1.0–22.5	1.5–20	1.0–22.5	1.0–22.5
Reflns measd	6098	4743	7153	8012
Unique reflns	4979	3939	5548	6126
Obsd reflns	3583	1601	3608	2736
R	0.045	0.082	0.052	0.039
k	2.49	1.0	1.0	1.0
g	0.002	0.012	0.007	0.004
R_w	0.053	0.084	0.055	0.042

Table 6

Fractional atomic coordinates ($\times 10^5$ for Ru, 10^4 for other atoms) for $Ru_4(\mu\text{-}PPh)(\mu_4\text{-}PhC_2PPh_2)(\mu\text{-}CO)_2(CO)_8$ (3)

Atom	x	y	z
Ru(1)	45891(7)	19776(5)	16303(4)
Ru(2)	25047(7)	21239(4)	5797(4)
Ru(3)	8550(7)	12518(4)	11969(4)
Ru(4)	29582(7)	15184(4)	23749(4)
P(1)	2971(2)	978(1)	1263(1)
P(2)	14(2)	2350(2)	1514(1)
C(11)	5702(11)	2801(7)	1868(6)
O(11)	6359(8)	3314(5)	1981(5)
C(12)	5955(10)	1394(6)	1514(5)
O(12)	6778(8)	1055(5)	1437(4)
C(13)	4250(10)	2389(6)	546(5)
O(13)	4942(7)	2601(4)	227(4)
C(14)	4819(11)	1684(6)	2706(5)
O(14)	5694(8)	1655(5)	3172(4)
C(21)	1746(10)	3010(6)	126(5)
O(21)	1290(9)	3513(5)	−170(4)
C(22)	2148(11)	1609(6)	−252(5)
O(22)	1944(9)	1285(5)	−754(4)
C(31)	231(12)	405(7)	1571(7)
O(31)	−133(10)	−94(6)	1800(6)
C(32)	−101(12)	989(7)	324(7)
O(32)	−642(10)	862(6)	−210(5)
C(41)	2805(12)	601(6)	2770(5)
O(41)	2729(13)	18(5)	3038(5)
C(42)	2626(10)	1965(6)	3177(6)
O(42)	2494(9)	2183(5)	3668(4)
C(1)	2827(9)	2607(5)	1671(5)
C(2)	1636(8)	2270(5)	1570(4)
C(3)	2975(6)	3421(3)	1889(3)
C(4)	2553(6)	3668(3)	2450(3)
C(5)	2583(6)	4432(3)	2610(3)
C(6)	3036(6)	4951(3)	2209(3)
C(7)	3458(6)	4705(3)	1647(3)
C(8)	3428(6)	3940(3)	1487(3)
C(111)	3550(11)	63(6)	1086(4)
C(112)	3717(11)	−106(6)	440(4)
C(113)	4126(11)	−820(6)	304(4)
C(114)	4366(11)	−1367(6)	814(4)
C(115)	4199(11)	−1199(6)	1460(4)
C(116)	3791(11)	−484(6)	1596(4)
C(211)	−685(8)	3103(4)	939(4)
C(212)	−1689(8)	2929(4)	389(4)
C(213)	−2237(8)	3491(4)	−70(4)
C(214)	−1783(8)	4227(4)	23(4)
C(215)	−779(8)	4401(4)	573(4)
C(216)	−230(8)	3839(4)	1031(4)
C(221)	−435(7)	2452(3)	2311(3)
C(222)	−616(7)	3154(3)	2582(3)
C(223)	−949(7)	3201(3)	3204(3)
C(224)	−1101(7)	2546(3)	3556(3)
C(225)	−919(7)	1844(3)	3286(3)
C(226)	−586(7)	1797(3)	2663(3)
O(s)	4377(7)	4339(4)	9667(4)
C(s)	4525(36)	5063(6)	9640(18)

Table 7

Fractional atomic coordinates ($\times 10^4$) for $Ru_5(\mu_4\text{-PPh})\{\mu_3\text{-CCPh}(PPh_2)\}(CO)_{12}$ (6)

Atom	x	y	z
Ru(1)	2997(2)	2315(3)	4626(2)
Ru(2)	1896(2)	5056(3)	4595(2)
Ru(3)	1608(2)	2966(3)	4965(2)
Ru(4)	3324(2)	4438(3)	4189(2)
Ru(5)	2919(2)	3983(3)	5612(2)
P(1)	2173(6)	3560(9)	3930(6)
P(2)	2535(7)	915(9)	5221(8)
C(1)	4002(30)	2122(41)	4998(31)
O(1)	4605(18)	2055(24)	5310(17)
C(2)	3126(26)	1597(36)	3783(28)
O(2)	3285(18)	1057(27)	3305(20)
C(3)	1433(27)	5577(38)	3760(28)
O(3)	1137(20)	6062(30)	3233(22)
C(4)	1064(36)	5526(51)	5138(36)
O(4)	646(21)	5790(29)	5469(22)
C(5)	3172(25)	5176(36)	3357(28)
O(5)	3091(20)	5657(28)	2784(21)
C(6)	2497(24)	6238(34)	4887(24)
O(6)	2832(19)	6938(29)	5148(19)
C(7)	849(30)	3438(41)	5554(32)
O(7)	554(20)	3675(28)	6042(21)
C(8)	887(24)	2228(34)	4455(24)
O(8)	407(22)	1710(30)	4222(21)
C(9)	4118(25)	3732(34)	3879(25)
O(9)	4531(18)	3259(25)	3570(18)
C(10)	3962(31)	5279(44)	4790(31)
O(10)	4394(21)	5884(30)	5068(20)
C(11)	3895(37)	4142(49)	6036(37)
O(11)	4471(22)	4137(29)	6426(21)
C(12)	2503(26)	4699(35)	6363(28)
O(12)	2201(21)	5116(28)	6798(23)
C(13)	1790(12)	3298(22)	2974(17)
C(14)	2266(12)	3216(22)	2420(17)
C(15)	1967(12)	3096(22)	1673(17)
C(16)	1192(12)	3058(22)	1480(17)
C(17)	716(12)	3140(22)	2034(17)
C(18)	1015(12)	3260(22)	2781(17)
C(19)	2100(25)	1826(35)	5815(26)
C(20)	2634(23)	2604(34)	5658(25)
C(21)	1772(22)	1673(29)	6558(22)
C(22)	1180(22)	986(29)	6575(22)
C(23)	861(22)	842(29)	7236(22)
C(24)	1133(22)	1384(29)	7880(22)
C(25)	1725(22)	2070(29)	7863(22)
C(26)	2044(22)	2215(29)	7202(22)
C(27)	1908(18)	−59(21)	4736(19)
C(28)	1619(18)	93(21)	3989(19)
C(29)	1126(18)	−620(21)	3625(19)
C(30)	921(18)	−1485(21)	4007(19)
C(31)	1210(18)	−1636(21)	4753(19)
C(32)	1704(18)	−923(21)	5118(19)
C(33)	3282(18)	176(23)	5805(20)
C(34)	3495(18)	462(23)	6547(20)
C(35)	4084(18)	−43(23)	6972(20)
C(36)	4460(18)	−834(23)	6656(20)
C(37)	4247(18)	−1120(23)	5914(20)
C(38)	3658(18)	−615(23)	5488(20)

Table 8

Fractional atomic coordinates ($\times 10^5$ for Ru, $\times 10^4$ for other atoms) for $Ru_5(\mu_3\text{-}H)(\mu_4\text{-}PPh)\{(\mu_4\text{-}CCPh(C_6H_4)\}(\mu_3\text{-}PPh)(CO)_{10}$ (7)

Atom	x	y	z
Ru(1)	43404(7)	10211(9)	41762(3)
Ru(2)	39817(7)	11662(8)	31342(3)
Ru(3)	25494(7)	−416(9)	36520(3)
Ru(4)	24800(7)	23674(9)	39692(3)
Ru(5)	29957(7)	33386(9)	31369(3)
P(1)	4221(2)	2728(3)	3738(1)
P(2)	2731(3)	635(3)	4371(1)
C(1)	5340(11)	−294(13)	4290(4)
O(1)	5898(8)	−1041(9)	4329(4)
C(2)	5031(10)	1871(13)	4675(4)
O(2)	5416(9)	2421(10)	4971(4)
C(3)	3763(11)	−184(11)	2759(5)
O(3)	3622(9)	−961(10)	2516(4)
C(4)	5421(10)	1185(14)	3071(5)
O(4)	6266(9)	1166(10)	3049(4)
C(5)	1168(11)	−557(14)	3590(5)
O(5)	330(9)	−882(11)	3595(4)
C(6)	2958(11)	−1676(14)	3713(6)
O(6)	3192(12)	−2632(12)	3775(7)
C(7)	2682(11)	3465(14)	4447(5)
O(7)	2827(10)	4150(13)	4740(4)
C(8)	997(12)	2555(12)	3945(5)
O(8)	120(8)	2653(11)	3938(4)
C(9)	2143(10)	4562(13)	3335(5)
O(9)	1681(9)	5331(10)	3452(4)
C(10)	3910(13)	4627(15)	3009(5)
O(10)	4432(10)	5383(11)	2919(4)
C(11)	2406(9)	1481(11)	3239(4)
C(12)	1748(9)	2003(10)	2875(4)
C(13)	2285(10)	2316(11)	2484(4)
C(14)	3404(9)	2238(10)	2558(4)
C(15)	3950(11)	2554(11)	2205(4)
C(16)	3446(14)	3003(13)	1800(5)
C(17)	2368(16)	3103(17)	1731(5)
C(18)	1744(11)	2789(14)	2056(4)
C(19)	590(7)	2165(6)	2847(4)
C(20)	−6(7)	1122(6)	2825(4)
C(21)	−1089(7)	1194(6)	2772(4)
C(22)	−1576(7)	2310(6)	2741(4)
C(23)	−981(7)	3354(6)	2763(4)
C(24)	102(7)	3281(6)	2817(4)
C(25)	5166(8)	3880(8)	3911(4)
C(26)	6208(8)	3668(8)	3867(4)
C(27)	6945(8)	4569(8)	3975(4)
C(28)	6640(8)	5681(8)	4125(4)
C(29)	5598(8)	5893(8)	4169(4)
C(30)	4861(8)	4993(8)	4061(4)
C(31)	2128(9)	193(7)	4858(4)
C(32)	1570(9)	1012(7)	5086(4)
C(33)	1133(9)	654(7)	5470(4)
C(34)	1256(9)	−522(7)	5626(4)
C(35)	1814(9)	−1341(7)	5398(4)
C(36)	2250(9)	−983(7)	5014(4)

Table 9

Fractional atomic coordinates ($\times 10^4$) for $Ru_5(\mu_4\text{-PPh})\{\mu_4\text{-CCPh}(C_6H_4)\}\{\mu\text{-PPh(OMe)}\}(CO)_{11}$ (12)

Atom	x	y	z
Ru(1)	2579(1)	913(1)	3435(1)
Ru(2)	2651(1)	−1706(1)	3363(1)
Ru(3)	2662(1)	−165(1)	2255(1)
Ru(4)	1417(1)	301(1)	2524(1)
Ru(5)	1241(1)	−2167(1)	2958(1)
P(1)	1688(2)	−454(4)	3566(2)
P(2)	3444(2)	−317(4)	3725(2)
C(1)	2877(9)	2536(17)	3256(9)
O(1)	3047(9)	3526(14)	3185(9)
C(2)	2557(8)	1551(16)	4266(10)
O(2)	2582(7)	1886(14)	4760(6)
C(3)	3197(8)	−2928(15)	3048(8)
O(3)	3534(6)	−3671(12)	2902(6)
C(4)	2755(8)	−2566(15)	4132(8)
O(4)	2821(6)	−3086(12)	4595(6)
C(5)	3468(9)	−876(15)	2127(8)
O(5)	3957(5)	−1337(12)	2046(6)
C(6)	3060(8)	1372(18)	2128(8)
O(6)	3325(6)	2243(12)	1985(7)
C(7)	1319(9)	2057(19)	2608(8)
O(7)	1242(7)	3097(14)	2662(8)
C(8)	519(9)	162(16)	2227(9)
O(8)	−23(7)	45(12)	2026(7)
C(9)	741(9)	−2959(16)	2183(9)
O(9)	447(7)	−3333(16)	1761(6)
C(10)	1471(9)	−3664(17)	3364(8)
O(10)	1603(7)	−4618(14)	3603(6)
C(11)	472(9)	−2043(17)	3366(9)
O(11)	10(6)	−1891(14)	3581(7)
C(12)	4095(9)	370(23)	4806(9)
O(12)	3671(5)	−496(11)	4486(5)
C(13)	1887(7)	−1494(14)	2403(7)
C(14)	2079(6)	−1759(14)	1816(7)
C(15)	1947(7)	−681(15)	1365(7)
C(16)	1700(7)	423(14)	1644(7)
C(17)	1610(8)	1486(15)	1234(9)
C(18)	1714(8)	1491(18)	635(8)
C(19)	1899(9)	367(18)	368(8)
C(20)	2024(7)	−712(14)	731(7)
C(21)	2361(5)	−2952(8)	1623(5)
C(22)	2808(5)	−2964(8)	1195(5)
C(23)	3034(5)	−4099(8)	990(5)
C(24)	2814(5)	−5222(8)	1215(5)
C(25)	2368(5)	−5210(8)	1643(5)
C(26)	2142(5)	−4075(8)	1847(5)
C(27)	1356(5)	−237(9)	4293(6)
C(28)	1440(5)	−1162(9)	4754(6)
C(29)	1168(5)	−1007(9)	5305(6)
C(30)	813(5)	73(9)	5395(6)
C(31)	729(5)	997(9)	4933(6)
C(32)	1001(5)	843(9)	4382(6)
C(33)	4242(5)	−232(9)	3455(6)
C(34)	4452(5)	843(9)	3176(6)

continued

Table 9 (continued)

Atom	x	y	z
C(35)	5065(5)	862(9)	2973(6)
C(36)	5468(5)	−193(9)	3049(6)
C(37)	5258(5)	−1267(9)	3327(6)
C(38)	4645(5)	−1287(9)	3530(6)
O(13)	5423(16)	11764(33)	9489(16)
O(14)	16(11)	5752(22)	5482(11)
C(39)	199(18)	5843(34)	4877(12)
O(15)	6050(24)	9333(41)	9434(22)
C(40)	5456(28)	9688(59)	9057(28)

A major base-line was also observed in the original TLC separation of the reaction product.

Crystallography. Intensity data for **3**, **6**, **7** and **12** were measured at room temperature on an Enraf–Nonius CAD4F diffractometer fitted with graphite-monochromated Mo-K_α radiation, λ 0.7107 Å. The $\omega/2\theta$ scan technique was employed in each case. The data sets were corrected routinely for Lorentz and polarisation effects [28] as well as for absorption with the use of an analytical procedure. Relevant crystal data are given in Table 5.

The structures were solved by direct methods and each refined by a full-matrix least-squares procedure based on F [29]. Non-hydrogen and non-phenyl carbon atoms were refined with anisotropic thermal parameters for **3**, **7** and **12**, whereas for **6**, only the Ru and P atoms were refined anisotropically. Phenyl rings were refined as hexagonal rigid groups with individual isotropic thermal parameters. For **3** and **12**, hydrogen atoms were included in their calculated positions. For **3**, a disordered molecule of MeOH was located and refined. Similarly, for **12**, one H_2O and two MeOH molecules of crystallisation were refined. A weighting scheme of the form $w = k/[\sigma^2(F) + g(F)^2]$ was included for each refinement and the refinements were continued until convergence. Final refinement details are given in Table 5.

Scattering factors for C, H, O and P were those incorporated in SHELX while those for neutral Ru were from ref. 30, the values being corrected for f' and f''. The diagrams shown in Fig. 2–4 and 6 were drawn with ORTEP [31] with 15% probability ellipsoids. Fractional atomic coordinates for **3**, **6**, **7** and **12** are listed in Tables 6–9, respectively.

Supplementary material. Tables of anisotroic thermal parameters for **3**, **6**, **7** and **12**, all bond distances and angles, and hydrogen atom parameters for **3** and **12** (22 pages), and lists of observed and calculated structure factors for **3**, **6**, **7** and **12**. (33 pages). are available from the authors.

Acknowledgements

We thank the Australian Research Council for grants in support of this work. MJL held a Commonwealth Post-Graduate Research Award.

References

1 Part LXII: M.I. Bruce, M.J. Liddell, M.L. Williams, B.K. Nicholson, Organometallics, in press.
2 M.I. Bruce, M.L. Williams, J.M. Patrick, A.H. White J. Chem. Soc., Dalton Trans., (1985) 1229.
3 M.I. Bruce, M.L. Williams, B.W. Skelton, A.H. White, J. Organomet. Chem., 369 (1989) 393.
4 (a) M.I. Bruce, M.L. Williams, J. Organomet. Chem., 282 (1985) C11; (b) M.I. Bruce, M.R. Snow, E.R.T. Tiekink, M.L. Williams, J. Chem. Soc., Chem. Commun., (1986) 701.
5 M.I. Bruce, J. Organomet. Chem., Jom 20765.
6 J.-C. Daran, Y. Jeannin, O. Kristiansson, Organometallics, 4 (1985) 1882.
7 L.D. Detter, O.W. Hand, R.G. Cooks, R.A. Walton, Mass Spectrom. Rev., 7 (1988) 465.
8 A.J. Carty, A.A. Cherkas, L.H. Randall, Polyhedron, 7 (1988) 1045.
9 D. Astruc, Angew. Chem., 100 (1988) 662; Angew. Chem., Int. Ed. Engl., 27 (1988) 634.
10 J.S. Field, R.J. Haines, E. Minshall, D.N. Smit, J. Organomet. Chem., 310 (1986) C69.
11 (a) T. Jaeger, S. Aime, H. Vahrenkamp, Organometallics, 5 (1986) 245; (b) H.H. Ohst, J.K. Kochi, Organometallics, 5 (1986) 1359.
12 J.-F. Halet, J.-Y. Saillard, New J. Chem., 11 (1987) 315; and ref. cited therein.
13 J.S. Field, R.J. Haines, D.N. Smit, K. Natarajan, O. Scheidsteger, G. Huttner, J. Organomet. Chem., 240 (1982) C23.
14 M.I. Bruce, A.G. Swincer, Adv. Organomet. Chem., 22 (1983) 59.
15 S.A. MacLaughlin, N.J. Taylor, A.J. Carty, Organometallics, 2 (1983) 1194.
16 K. Kwek, N.J. Taylor, A.J. Carty, J. Am. Chem. Soc., 106 (1984) 4636
17 A.J. Carty, Pure Appl. Chem., 54 (1982) 113.
18 P. Vierling, J.G. Reiss, A. Grand, J. Am. Chem. Soc., 103 (1981) 103, 2466.
19 (a) D.H. Farrar, P.F. Jackson, B.F.G. Johnson, J. Lewis, J.N. Nicholls, J. Chem. Soc., Chem. Commun, (1981) 415; (b) B.F.G. Johnson, J. Lewis, J.N. Nicholls, I.A. Oxton, P.R. Raithby, J. Chem. Soc., Chem. Commun., (1982) 289; (c) B.F.G. Johnson, J. Lewis, J.N. Nicholls, J. Puga, P.R. Raithby, M.J. Rosales, J. Chem. Soc., Dalton Trans., (1983) 277.
20 (a) C.W. Bradford, R.S. Nyholm, G.J. Gainsford, J.M. Guss, P.R. Ireland, R. Mason, J. Chem. Soc., Chem. Commun., (1972) 87; (b) G.J. Gainsford, J.M. Guss, P.R. Ireland, R. Mason, C.W. Bradford, R.S. Nyholm, J. Organomet. Chem., 40 (1972) C70; (c) C.W. Bradford, R.S. Nyholm, J. Chem. Soc., Dalton Trans., (1973) 529.
21 M.R. Churchill, F.J. Hollander, Inorg. Chem., 18 (1979) 161.
22 G. Huttner, K. Knoll, Angew. Chem., 99 (1987) 765; Angew. Chem., Int. Ed. Engl., 26 (1987) 743.
23 A.J. Carty, S.A. MacLaughlin, D. Nucciarone, in J.G. Verkade, L.D. Quin, (Eds.) Phosphorus-31 NMR Spectroscopy in Stereochemical Analysis: Organic Compounds and Metal Complexes, VCH Publishers, New York 1986, Chapter 16.
24 K. Natarajan, L. Zsolnai, G. Huttner, J. Organomet. Chem., 209 (1981) 85.
25 J.S. Fields, R.J. Haines, D.N. Smit, J. Chem. Soc., Dalton Trans., (1988) 1315.
26 M.I. Bruce, J.G. Matisons, B.K. Nicholson, J. Organomet. Chem., 243 (1983) 321.
27 M.I. Bruce, M.P. Cifuentes, M.R. Snow, E.R.T. Tiekink, J. Organomet. Chem., 359 (1989) 379.
28 PREABS and PROCES: Data reduction programs for the CAD4 diffractometer, University of Melbourne, 1981.
29 G.M. Sheldrick, SHELX, Programme for crystal structure determination, University of Cambridge, Cambridge, 1976.
30 J.A. Ibers, W.C. Hamilton (Eds.), International Tables for X-Ray Crystallography, Kynoch, Birmingham, 1974, Vol. 4, p. 99, 149.
31 C.K. Johnson, ORTEP II, Report ORNL-3794, Oak Ridge National Laboratory, Oak Ridge, TN.
32 J.S. Field, R.J. Haines and D.N. Smit, J. Chem. Soc., Dalton Trans., (1988) 1315.